Utrecht University

MSc. Thesis

Mathematical Sciences

Capital Valuation Adjustment for Bermudan Options by the Stochastic Grid Bundling Method

Author:

Marcus W. F. M. Bannenberg

Supervisors:

dr. K. Dajani
Utrecht University

prof. dr. ir. C.W. Oosterlee
Centrum Wiskunde en Informatica

Daily supervisors:

dr. H. van Leeuwen
Deloitte FRM

S. Kampen, MSc
Deloitte FRM

Second reader:

dr. P.A. Zegeling
Utrecht University

August 2018

Acknowledgements

First and foremost I would like to express my sincere gratitude to Dr K. Dajani, Prof. C.W. Oosterlee and Dr P.A. Zegeling. Thank you for taking the time to guide me during my research process and for inspiring me to continue my research aspirations.

I am very thankful for the opportunity provided by Deloitte, and especially the Financial Risk Management department, to write my thesis in their superb working environment. Thank you S. Kampen and Dr H. van Leeuwen for the insights and endless knowledge of financial risk.

Finally I would like to thank my loving parents and sister for their unwavering support along the way and helping me achieve my goals. I would not have succeeded without you.

Marcus W. F. M. Bannenberg
Utrecht, August 2018

Contents

I

Introduction

Financial derivatives have been around ever since people exchanged goods and services. The first derivatives were instruments to protect against harvest failure or facilitate the trade of commodities. These contracts were defined as agreements based on an underlying asset. Instead of the immediate trade of this underlying asset, the derivative contract defines agreements to exchange other assets, e.g. cash, for the underlying asset during a specific time horizon. The fact that these types of contracts have been around for a long time can be illustrated by the following example, as given by Don Chance in [Cha08]: In the book of Genesis, around 1700 B.C., an option contract is struck between Jacob and Laban. This option stated that for the price of seven years of labour, the payoff would be that Jacob got to marry Laban's daughter Rachel. Since Laban did not fulfil his end of the bargain, he made Jacob marry Leah, his older daughter, this is also one of the first ever recorded default on a derivative.

Derivatives have come a long way since the contract between Jacob and Laban and the first derivatives exchange was created in Chicago in 1848, the Chicago Board of Trade, and is still operating. From 1865 on it created standardised futures contracts and later introduced a clearinghouse to reduce the counterparty risk, as well as the introduction of a margining system. [KP12]. Widespread use of derivatives started to gain momentum from the 1970's. With the introduction of the computer more sophisticated models could be used and quickly and efficiently computed. Then in 1973 Black and Scholes published their paper, [BS73], on option pricing and hedging which revolutionised the options market. Before the Black and Scholes model the option markets were quite small, only 911 options on opening day in 1973. Since then the option markets have expanded to over 20,000 in mid 1973 and to 100,000 in 1997. By now the option market is one of the largest and most active security market. The Black and Scholes model provided a valuation benchmark and a method for replicating or hedging the option positions. After this the next big step in derivatives trading was introduced in 1992 when the Chicago Mercantile Exchange introduced electronic trading [Mat10]. For the next decade markets were soaring, but then in 2007 the financial crisis hit.

The beginning of this financial crisis in 2007 marked the start of significant changes in the pricing of derivatives. In the years leading up to the crisis risks related to the interbank market were ignored. During the crisis the collapse of major banks which were previously considered "too big to fail", such as Lehman Brothers or Bear Stearns, introduced a major shift in the perception of the interbank funding and the risk involved. Pre-crisis banks considered their peers to be risk-free which, as shown by the Bear Stearns collapse, they were not. This caused that banks could no longer borrow and lend at a rate which risk term structure was considered non-material. Furthermore it was evident that there was a need for improved regulation and tighter risk controls if a new financial crisis were to be prevented.

This increase of new regulatory requirements were mainly aimed at the over-the-counter (OTC) derivatives market, due to the fact that this market contributed significantly to the financial crisis. As opposed to exchange-traded derivatives, which were already more regulated via clearing houses and exchanges. The Basel Comittee identified key shortcomings of the financial sector which are stated as apparent causes of the financial crisis. The main crisis trigger is identified as an excess of global liquidity and leverage while maintaining deficient capital of insufficient quality and meagre liquidity buffer. Furthermore the crisis was worsened by a deleveraging process and interconnectedness among the too-big-to-fail financial institutions. Other factors as insufficient risk management and lack of market transparency are also stated.

Before the Basel III regulations, exposure of derivatives to counter party credit risk was already accounted for in terms of a credit valuation adjustment, CVA, since this was already included in the accounting regulations, e.g. IFRS states that this is part of the fair value. However, the changes in the credit spreads of the banks, caused by the change in interbank funding, caused huge changes in the CVA part of this fair value. These changes in the CVA drastically impacted banks financially, without many actual counterparty defaults. Therefore Basel III introduced a requirement for banks to hold regulatory capital for these influxes in CVA. This required capital is known as the CVA capital charge.

For instance counterparty credit risk and liquidity risk played a major role in this contribution. Since then the new regulations by Basel III state that financial institutions should charge Credit Value Adjustment (CVA) to their counterparties for OTC trades. The CVA was only the first of many value adjustments and gave rise to a whole pantheon such as, DVA (debit value adjustment), FVA (funding value adjustment) and many more. These value adjustment terms are generally referred to as an X-Value Adjustment (XVA).

The focus of this thesis lies on the value adjustment related to the regulatory capital that needs to be held during the lifetime of the derivative. This value adjusmtent is known as the capital valuation adjustment, KVA, as this adjustment contains interesting computational challenges. As opposed to the calculation of for instance CVA or FVA the calculation of KVA contains the need to forecast the future prices at each time step. In a standard approach this would result in a heavily nested Monte Carlo simulation situation, which is very computationally heavy.

In an effort to solve these computational challenges for the KVA pricing of a basic EUR/USD FX forward portfolio the Stochastic Grid Bundling Method, SGBM, is applied by Jain, Karlsson and Kandhai in [JKK17]. The SGBM was originally developed by Jain and Oosterlee in [JO15] to price Bermudan options and their Greeks efficiently. This method approximates the pricing problem through a regression type approach to the valuation of derivatives. This approach makes it possible to calculate expectations under different measures without resulting in a nested simulations situation. This thesis continues the efforts of Jain, Karlsson and Kandhai, and aims to price the KVA term related to the counterparty credit risk for Bermudan options under Multidimensional-Black-and-Scholes and Heston dynamics.

Thesis organisation

The thesis continues with the second chapter by constructing a mathematical framework for the pricing of derivatives. This is done through a literature analysis of the publication by Green and Kenyon, [GKD14][GK15], which in itself rests on the work of Burgard and Kjaer, [BK11].

The third chapter discusses the origin and specifics of the regulations and construction of the regulatory capital that needs to be held during the lifetime of a derivative. Since the focus of this thesis lies on the value adjustment related to the counterparty credit risk term of the regulatory capital, only this aspect will be discussed. A short note on the market risk- and CVA-part of the regulatory capital is given in the outlook section of the last chapter.

Chapter four presents the SGBM as numerical method for the pricing of Bermudan options and elaborates on the Least Squares Method, LSM, which will be used as a Benchmark for the SGBM. Multiple aspects of the SGBM algorithm are covered such as specific bundling techniques and the characteristic function of the conditional expectation. The two algorithms are tested for convergence against different types of dynamics, both with and without stochastic volatility.

With all the tools in the toolbox for calculating all the aspects of the KVA term the fifth chapter presents the main results of this thesis related to the pricing of the KVA. A fully nested Monte Carlo algorithm could be used to verify these results, but due to exorbitant computational costs this could not be included in this thesis.

The thesis ends with the sixth chapter with a wrap up of the previous chapters. There, a short synopsis is given of the work done in this research project and the main results. Then lastly an outlook for further research is presented.

II

Derivative pricing theory

In this chapter the mathematical foundations are laid out for the pricing of options and their value adjustments. Through the basic concepts of stochastic calculus a mathematical framework comparable to the Black and Scholes framework is constructed by means of a partial differential approach and a replicating portfolio. This is then extended to include counterparty credit risk and a number of other real-world concepts such as funding, collateral and capital. This chapter provides mathematical expressions for the calculation of the value adjustments related to various types of XVA such as regulatory capital (KVA) and initial margin (MVA) while maintaining generality on the explicit calculation techniques used for the implementation.

2.1 Introduction

Before discussing simulation based methods for the pricing of derivatives, it is essential to construct the mathematical framework which makes this possible. This chapter provides a step by step approach to the derivation of the derivative pricing theory. The derivation of this theory follows that of [Pen08], whereas the proofs for the theorems and lemmata can be found in [Øks03] and are omitted here. The chapter starts with the mathematical foundations based in stochastic calculus. From there the basic Black and Scholes partial differential equation is derived and the risk-free derivative pricing formula by means of a replicating portfolio. Then the framework is extended to the one described by [GK15] to include real-world events such as defaults, funding, collateral, capital and such.

To start with the definition of a mathematical theory for derivatives pricing first a definition of a derivative is needed. A derivative is defined as a financial contract which has its cash flows derived from an underlying variable, be it interest rate, asset price or other types of observable variables. This chapter focuses on derivatives related to underlying asset prices, such as options, futures or forwards. For now the derivative remains an abstract object to keep the pricing theory general. Further on explicit types of derivatives will be discussed. For the derivative pricing theory the derivative is assumed to have at least a maturity time, T, and a payoff function h depending on the underlying.

2.2 A mathematical pricing framework

The definition of a mathematical pricing framework is performed through several steps. First a setup of the pricing environment is given through key concepts of stochastic calculus such as Brownian motions and Itô's lemma. Then a basic framework is constructed based on some simple assumptions and then the concept of risk-free pricing is derived.

2.2.1 The environment

For the construction of a derivative pricing framework one first needs to define the environment in which the derivative pricing takes place. To define this environment one starts with a probability space.

Definition 2.2.1 – Probability space. *The triple $(\Omega, \mathcal{F}, \mathbb{P})$, comprising of a state space Ω, a σ-algebra $\mathcal{F}$ of subsets of Ω, and a probability measure $\mathbb{P}$ on $(\Omega, \mathcal{F})$ is called a probability space.*

Let $(\Omega, \mathcal{F}, \mathbb{P})$ be the probability space in which we model the real-world behaviour of the underlying assets of the derivative. The behaviour of the underlying asset is modelled by a stochastic process, which will be discussed in more detail in the coming subsections.

Definition 2.2.2 – Stochastic Process. *A stochastic process is a family of random variables $\{S_t\}$ defined on a given probability space, indexed by t, with t in index set T.*

2.2.2 The information

To model the market information that is known up to time t a filtration, $\{\mathcal{F}_t\}_{0 \leq t \leq T}$, is constructed by using the σ-algebra $\mathcal{F}$ of the probability space.

Definition 2.2.3 – σ-algebra. *Let Ω be a set and let 2^Ω be its power set. Then a subset $\mathcal{F} \subseteq 2^\Omega$ is a σ-algebra if the following statements are satisfied.*

- *$\mathcal{F}$ contains the empty-set, $\emptyset \in \mathcal{F}$.*
- *$\mathcal{F}$ is closed under complements, $\forall A \in \mathcal{F} : (\Omega \backslash A) \in \mathcal{F}$.*
- *$\mathcal{F}$ is closed under countable unions, $\forall A_1, A_2, ... \in \mathcal{F} : \bigcup_{i=1}^{\infty} A_i \in \mathcal{F}$.*

Definition 2.2.4 – Filtration. *Let $(\Omega, \mathcal{F}, \mathbb{P})$ be a probability space. Then a non-decreasing family, $\{\mathcal{F}_t\}_{0 \leq t \leq T}$, consisting of sub σ-algebras of $\mathcal{F}$ that satisfies*

$$\mathcal{F}_u \subset \mathcal{F}_t \subset \mathcal{F}_T, 0 \leq u < t \leq T,$$

is called a filtration. Here $\mathcal{F}_t$ represents the information that is available at time t.

In the framework $\mathcal{F}_t$ represents the market information that is known at time t and $\{\mathcal{F}_t\}_{0 \leq t \leq T}$ the information flow throughout time. Furthermore if all random variables S_t are measurable under $\mathcal{F}_t$, this stochastic process is considered to be adapted.

Definition 2.2.5 – Adapted process. *Given probability space $(\Omega, \mathcal{F}, \mathbb{P})$ and index set $[0, T]$. Let $\{\mathcal{F}_t\}_{0 \leq t \leq T}$, be a filtration on the σ-algebra $\mathcal{F}$ and $\{S_t\}$ a stochastic process. Then if all random variables S_t are measurable under $\mathcal{F}_t$ the process $\{S_t\}$ is adapted.*

The smallest filtration for which a stochastic process is a adapted is called a natural filtration. This natural filtration can be generated by the stochastic process $\{S_t\}_{0 \leq t \leq T}$ through a family of σ-algebras. This natural filtration is a representation of the accumulated information generated by the stochastic process up until time t.

Definition 2.2.6 – NATURAL FILTRATION. *Let* $(\Omega, \mathcal{F}, \mathbb{P})$ *be a probability space. Then*

$$\mathcal{F}_t = \sigma(\{S_u^{-1}(B) : u \leq t, B \in \mathcal{B}\}),$$

with $\mathcal{B}$ *the Borel* σ*-algebra, is called the natural filtration associated with the process* $\{S_t : t \geq 0\}$.

2.2.3 THE UNDERLYING ASSETS

With the probability space and information flow defined let us elaborate on a specific stochastic process that governs the dynamics of the underlying assets in the underlying probability space, the process of a Brownian motion.

Definition 2.2.7 – BROWNIAN MOTION. *A continuous time stochastic process* $(W_t \ t \geq 0)$ *that satisfies* $W_0 = 0$ *and has independent Gaussian increments*

$$\forall t \geq 0, W_{t+\delta} - W_t, \delta \geq 0 \text{ is independent of } W_s, s \leq t, \text{ and } W_{t+\delta} - W_t \sim \mathcal{N}(0, \delta).$$

is called a Brownian motion.

An important aspect of a Brownian motion $\{W_t\}$ is that it is a martingale when $\{W_t\}$ is adapted to the filtration $\{\mathcal{F}_t\}_{t \leq t \leq T}$, this property is used later in the definition of the risk-free pricing formula.

Definition 2.2.8 – MARTINGALE. *A stochastic process* $\{S_t\}$*, on probability space* $(\Omega, \mathcal{F}, \mathbb{P})$ *and associated with filtration* $\{\mathcal{F}_t\}_{0 \leq t \leq T}$*, is considered a martingale if the following statements are satisfied.*

- $\{S_t\}$ *is adapted to the filtration* $\mathcal{F}_t$.
- *The expectation of the absolute value of the process is finite,* $\mathbb{E}[|S_t|] < \infty, \forall t$.
- $\mathbb{E}[S_u|\mathcal{F}_t] = S_t, \forall u \geq t \geq 0$.

From the definition, a martingale is thus a process that, given the information up to time t, has an expectation for time u equal to the state in time t. An extension of the Brownian motion can be made and is called a geometric Brownian motion. The geometric Brownian motion has a drift parameter, μ and a volatility parameter σ, which are both set to a constant in the Black and Scholes framework. Since this process remains positive if S_t starts at a positive value it is often used to model the price of stocks, equities or commodities.

Definition 2.2.9 – GEOMETRIC BROWNIAN MOTION. *The continuous time stochastic process* S_t *that satisfies the stochastic differential equation*

$$dS_t = \mu S_t dt + \sigma S_t dW_t, \tag{2.1}$$

is called a geometric Brownian motion.

If the geometric Brownian motion is adapted to a filtration, then the stochastic process is classified as an Itô process.

Definition 2.2.10 – ITÔ PROCESS. *An adapted stochastic process* $\{S_t\}$ *on probability space* $(\Omega, \mathcal{F}, \mathbb{P})$ *and associated with filtration* $\{\mathcal{F}_t\}$ *which can be written in the form*

$$dS_t = \mu_t dt + \sigma_t dW_t,$$

is called an Itô process. Where S_0 *is deterministic and for which* μ_t *and* σ_t *are adapted processes.*

To obtain the differential of an Itô process a powerful stochastic tool is used, namely Itô's lemma. This lemma will be used repeatedly therefore the formal definition is given below.

Theorem 2.2.1 – Itô's Lemma. *Let $\{S_t\}$ be an Itô process which follows the stochastic differential equation $dS_t = \mu(S_t,t)dt + \sigma(S_t,t)dW_t$ and let $F(S_t,t)$ be an at least twice differentiable function. Then the differential of $F(S_t,t)$ is given by*

$$dF = \frac{\partial F}{\partial dS_t}dS_t + \frac{\partial F}{\partial t}dt + \frac{1}{2}\frac{\partial^2 F}{\partial S_t^2}(dS_t)^2,$$

where the product $(dS_t)^2 = \sigma(S_t,t)^2 dt$. Which results in

$$dF = \left[\frac{\partial F}{\partial S_t}\mu(S_t,t) + \frac{\partial F}{\partial t} + \frac{1}{2}\frac{\partial^2 F}{\partial S_t^2}\sigma^2(S_t,t)\right]dt + \frac{\partial F}{\partial S_t}\sigma(S_t,t)dW_t.$$

2.2.4 The risk-neutral rate

Another ingredient needed for the pricing of derivatives is the notion of the time value of money. Another asset is introduced into the pricing framework, namely a risk-neutral asset. This asset can be seen as money that is deposited into a savings account. In the pricing framework this asset is assumed to exist. The process B_t denotes the value of the asset at time $t \in [0,T]$, and a continuously compounding convention is used to model this asset, as described by

$$dB_t = rB_t dt, \tag{2.2}$$

Where r is the interest rate, and is assumed to be constant. Solving Equation 2.2 results in the expression

$$B_t = e^{rt}B_0.$$

This deterministic formula describes the time value of money, or the rate at which money grows without any risk. Therefore this rate is called the risk-neutral rate.

2.2.5 The assumptions

To continue defining the mathematical framework, a couple of assumptions are made in the model. This section provides a description and definition of these assumptions. All future frameworks of this thesis rely on these assumptions unless stated otherwise. The assumptions stated below originate from the original Black and Scholes model, [BS73].

1. The risk-neutral interest rate, r, is known and is constant through time.

2. Let $(\Omega, \mathcal{F}, \mathbb{P})$ be a probability space. The asset price is an Itô process and more precisely a geometric Brownian motion.

   $$dS_t = \mu S_t dt + \sigma S_t dW_t. \tag{2.3}$$

   And the risk-free bank accounts dynamics are given by

   $$dB_t = rB_t dt,$$
   $$B_0 = 1.$$

   With the solution $B_t = e^{rt}B_0$.

3. There are no dividends or other distributions.

4. The markets are frictionless, i.e. costs and restrains associated with transactions are considered to be non-existent.

5. It is possible to borrow any fraction of the price of a security to buy it or to hold it, at the short-term interest rate.

6. There is no penalty on short selling. One can sell a security which one does not own by accepting the price of the security from the buyer and agree to settle with the buyer on a future date through paying the price of the security on that future date.

7. The market is arbitrage free, with the definition of arbitrage as a portfolio process Π_t, with $\Pi_0 = 0$, for which holds that

$$\mathbb{P}(\Pi_t \geq 0) = 1 \text{ and } \mathbb{P}(\Pi_t \neq 0) > 0.$$

2.2.6 Hedging

Consider a portfolio that consists of one shorted derivative, a position β_t in the underlying asset and a risk-free asset. This portfolio defines the position of a derivatives trader that has sold one derivative and hedges the derivatives risk by investing or borrowing capital at the risk-free rate and buying or selling some of the underlying assets. The portfolio is restricted to have a zero net investment and required to be self-financing.

Definition 2.2.11 – Self-financing. *A portfolio is considered self-financing if there is no exogenous infusion or withdrawal of money; the purchase of a new asset must be financed by the sale of an old one. The change in the value of the portfolio thus depends on the evolution of the price of the underlying asset and the risk-free bank account.*

Define Δ_t as the fraction of underlying assets in the portfolio. Due to the zero net investment restriction the fraction of the risk-free asset is $\beta_t = V_t - \Delta_t S_t$, with V_t the value of the derivative at time t, which is assumed to be twice differentiable. This assumption is later shown to be justified by the no arbitrage assumption. This expression for β_t implies that the return of this portfolio with value Π_t can be denoted by

$$d\Pi_t = -dV_t + \Delta_t dS_t + [V_t - \Delta_t S_t]rdt. \tag{2.4}$$

Since the derivative price is a function apply Itô's lemma and obtain

$$dV_t = \left[\frac{\partial V_t}{\partial S_t}\mu + \frac{\partial V_t}{\partial t} + \frac{1}{2}\frac{\partial^2 V_t}{\partial S_t^2}\sigma^2\right]dt + \frac{\partial V_t}{\partial S_t}\sigma dW_t \tag{2.5}$$

Plugging the asset dynamics 2.3 and 2.5 into 2.4 results in

$$\begin{aligned} d\Pi_t = &- \left[\frac{\partial V_t}{\partial S_t}\mu + \frac{\partial V_t}{\partial t} + \frac{1}{2}\frac{\partial^2 V_t}{\partial S_t^2}\sigma^2\right]dt + \frac{\partial V_t}{\partial S_t}\sigma dW_t \\ &+ \Delta_t(\mu S_t dt + \sigma S_t dW_t) + [Vt - \Delta_t S_t]rdt. \end{aligned} \tag{2.6}$$

Now a suitable choice for Δ_t has to be made in order to eliminate the risk this portfolio is exposed to. Let this hedge ratio be the local sensitivity of the derivatives value to the price of the underlying asset,

$$\Delta_t = \frac{\partial V_t}{\partial S_t}.$$

Note that since the value of the derivative has a nonlinear relation with the underlying this derivative is time dependent and can continuously vary. Plugging this hedge ratio into equation 2.6 gives

$$d\Pi_t = \left[-\frac{\partial V_t}{\partial t} - \frac{1}{2}\sigma^2 S_t^2 \frac{\partial^2 V_t}{\partial S_t^2} + rV_t - rS_t \frac{\partial V_t}{\partial S_t}\right] dt. \tag{2.7}$$

In this equation the term dW_t has dropped out which gives that it is entirely deterministic. The hedge ratio has thus successfully eliminated the risk from this portfolio. Therefore, to avoid arbitrage, the rate of return of this portfolio must equal the rate of return of the risk-free asset, r, and remain zero due to the zero net investment requirement. The rate of return thus satisfies

$$d\Pi_0 = r\Pi_0 dt = r0dt = 0 \implies \Pi_t = 0 \forall t.$$

With the insight obtained from the no arbitrage condition a partial differential equation is constructed by combining the previous equation and 2.7 into

$$\frac{\partial V_t}{\partial t} + \frac{1}{2}\sigma^2 S_t^2 \frac{\partial^2 V_t}{\partial S_t^2} + rS_t \frac{\partial V_t}{\partial S_t} - rV_t = 0. \tag{2.8}$$

Which is the classic Black and Scholes partial differential equation.

2.2.7 The market price of risk

To construct a more general pricing theory the assumptions made by Black and Scholes are slightly relaxed. Let $\{S_t\}$ be the stochastic process that describes a risky asset with the dynamics governed by

$$dS = \mu S_t dt + \sigma S_t dW_t, \tag{2.9}$$

but now $\mu = \mu(S_t, t)$ and $\sigma = \sigma(S_t, t)$ are functions that can depend on the asset and time. Again let V_t denote the value of a derivative. Then it follows from Itô's lemma that the dynamics of V_t satisfy

$$dV_t = \mu_V V_t dt + \sigma_V V_t dW_t. \tag{2.10}$$

with $\mu_V V_t = V_t + \mu S_t V_t + \frac{1}{2}\sigma S_t^2 \frac{\partial^2 V_t}{\partial S_t^2}$ and $\sigma_V V_t = \sigma S_t \frac{\partial V_t}{\partial S_t}$. Analogous to the previous section a portfolio is constructed which consists of one shorted derivative and fraction $\Delta_t = \frac{\partial V_t}{\partial S_t}$ of risk-free assets, therefore the dynamics are represented by

$$\begin{aligned} d\Pi_t &= -dV_t + \Delta_t dS_t, &(2.11)\\ &= -\mu_V V_t dt - \sigma_V V_t dW_t + \Delta_t \mu S_t dt + \sigma S_t \Delta_t dW_t, &(2.12)\\ &= (\Delta_t \mu S_t - \mu_V V_t)dt. &(2.13)\end{aligned}$$

As previously seen this portfolio has risk-free dynamics thus the following equality must hold

$$d\Pi = (\Delta_t \mu S_t - \mu_V V_t)dt = r\Pi_t dt = r(\Delta_t \mu S_t - \mu_V V_t)dt. \tag{2.14}$$

Which implies that

$$V_t \mu S_t - \mu_V V_t = r(-V_t + \frac{\partial V_t}{S_t} S_t). \tag{2.15}$$

Substitution into this equation the equality $\Delta_t = \frac{\sigma_V V_t}{\sigma S_t}$, see 2.9 gives that

$$\frac{\mu - r}{\sigma} = \frac{\mu_V - r}{\sigma_V} := \theta. \tag{2.16}$$

This is the so called market price of risk, which is unique under the no arbitrage assumption. From this, the dynamics of the derivative price are represented by

$$dV_t = (rV_t + \theta\sigma_V V_t)dt + \sigma_V V_t dW_t. \tag{2.17}$$

This shows that the drift term of the dynamics of the derivative price are dependent on the market price of risk θ. This poses a problem since this factor is not directly observable or estimated with ease. This problem is circumvented by changing the risk-measure from the real-world measure to the risk-neutral measure.

2.2.8 Risk neutral valuation

To change the probability measure, Girsanov's theorem is used. In general, this theorem states that the drift of a stochastic process can be changed if this process is interpreted under new probability measure.

Theorem 2.2.2 – Girsanov's theorem. *Consider a probability space* $(\Omega, \mathcal{F}, \mathbb{P})$ *and a Brownian motion* $\{W_t\}$ *with respect to* $\mathbb{P}$ *and associated filtration* $\{\mathcal{F}_t\}_{t\geq 0}$. *Let* $\{\theta_t\}$ *be a real valued stochastic process, adapted to* $\{\mathcal{F}_t\}_{t\geq 0}$. *Assume that*

$$\int_0^T \theta_t^2 dt < \infty.$$

Then the risk-neutral measure is defined as

$$\frac{d\mathbb{Q}}{d\mathbb{P}} = e^{-\theta W_T - \frac{1}{2}\theta^2 T}.$$

Set

$$\tilde{W}_t := W_t - \int_0^t \theta_u du, \quad t \in [0, T].$$

Then, for any $T > 0$ *the process* $\tilde{W}_t$ *is an* $\mathcal{F}_t$*-Brownian motion on the probability space* $(\Omega, \mathcal{F}, \mathbb{Q})$.

To apply this theorem define a new process $\tilde{W}_t = W_t + \int_0^t \theta du$, or in differential form $d\tilde{W} = dW_t + \theta dt$, and substitute this into equation 2.17 obtaining

$$\begin{aligned} dV_t &= (rV_t + \theta\sigma_V V_t)dt + \sigma_V V_t(d\tilde{W}_t - \theta dt), \\ &= rV_t dt + \sigma_V V_t d\tilde{W}_t. \end{aligned} \tag{2.18}$$

Now using that upon differentiation it holds that

$$d\left(\frac{V_t}{B_t}\right) = \frac{dV_t}{B_t} + V_t d(B_t^{-1}), \text{ and } \quad d\left(\frac{1}{B_t}\right) = -r\frac{1}{B_t}dt,$$

then it follows that the dynamics of the discounted portfolio are described by

$$\begin{aligned} d\left(\frac{V_t}{B_t}\right) &= \frac{dV_t}{B_t} + V_t d\left(\frac{1}{B_t}\right), \\ &= rB_t^{-1}dV_t dt - rB_t^{-1}V_t dt, \\ &= rB_t^{-1}V_t dt + \Delta_t\sigma_V\frac{S_t}{B_t}d\tilde{W}_t - rB_t^{-1}V_t dt, \\ &= \Delta_t\sigma_V\frac{V_t}{B_t}d\tilde{W}_t. \end{aligned}$$

This means that the discounted price process of the derivative is a drift-less process under the measure generated by $d\tilde{W}$, i.e. its expected change is zero. Therefore it is possible to express the expectation under the risk-neutral measure as

$$\frac{V_t}{B_t} = \mathbb{E}^{\mathbb{Q}}[\frac{V_T}{B_T}|\mathcal{F}_t]. \tag{2.19}$$

2.2.9 The replicating portfolio

Another way to obtain the risk-neutral price of a portfolio is by means of a replicating and self-financing portfolio, instead of the previously seen zero net investment portfolio. This portfolio continuously replicates the payoff of the derivative during the trade. Let Π_t be a portfolio that consists of fraction Δ_t, as in the previous section, units of the underlying asset, such that $\Pi_t = V_t$ holds, and $\Pi_t - \Delta_t S_t$ invested into the risk-free asset. The portfolio dynamics are then governed by

$$\begin{aligned}
d\Pi_t &= \Delta_t dS_t + r(\Pi_t - \Delta_t dV_t)dt, && (2.20)\\
&= \Delta_t[\mu S_t dt + \sigma S_t dW_t] + r(\Pi_t - \Delta_t dS_t)dt, && (2.21)\\
&= r\Pi_t dt + \Delta_t \sigma S_t \left[\theta dt + dW_t\right], && (2.22)\\
&= r\Pi_t dt + \Delta_t \sigma S_t d\tilde{W}_t, && (2.23)
\end{aligned}$$

Now it is evident from the previous section that through Itô's lemma the return of the discounted portfolio is given by

$$d\left(\frac{\Pi_t}{B_t}\right) = \Delta_t \sigma \frac{S_t}{B_t} d\tilde{W}_t.$$

Therefore under the risk-free measure $\mathbb{Q}$ and 2.19 it holds that

$$\Pi_t = \mathbb{E}^{\mathbb{Q}}[\frac{\Pi_T}{B_T}|\mathcal{F}_t] = \mathbb{E}^{\mathbb{Q}}[\frac{V_T}{B_T}|\mathcal{F}_t] = V_t. \tag{2.24}$$

Thus the payoff of the derivative at time t can be replicated by the self-financing portfolio.

2.3 Extension of the framework

A multitude of books, articles and publications have been written about the extension of the previously seen Black and Scholes framework to include counterparty credit risk, Piterbarg[Pit10], Lesniewski and Richter,[LR16], Burgard and Kjaer [BK13]. For this thesis the extension of the Black and Scholes PDE under the presence of bilateral counterparty credit risk, funding, collateral, capital and initial margin costs by Kenyon and Green is used [GK15].

This section is dedicated to the derivation of the XVA expressions following the Kenyon and Green semi-replication approach, a more detailed derivation is given in [Gre11].

Let $(\Omega, \mathcal{G}, \mathbb{P})$ be a probability space where $\{\mathcal{F}_t\}_{t\geq 0}$ is the market filtration generated by a Brownian motion $\{W_t\}$. Another filtration, $\{\mathcal{J}_t\}_{t\geq 0}$ models the default information. The enlarged filtration of $\{\mathcal{G}_t\}_{t\geq 0}$ is defined by $\mathcal{G}_t = \mathcal{F}_t \cup \mathcal{J}_t$, as in [LR16].

Consider two parties, a bank B and a counterparty C, which enter into a derivative trade, which has an economic value that is represented by $\hat{V}$. The total economic value contains the XVA-adjustments for counterparty credit risk and the funding costs, contrary to the value V in which these risks and costs are omitted. Therefore U is defined to be the total of XVA adjustment with

$$\hat{V} = V + U. \tag{2.25}$$

A semi-replication strategy is used to perfectly hedge out market factors and counterparty default. The difference with full-replication is that the semi-replication framework may not provide a perfect hedge on the default of B.

To apply the semi-replication strategy a portfolio is constructed consisting of a counterparty zero-coupon bond P_C with zero recovery, then two of the banks own bonds P_1 and P_2 which have different recoveries R_1 and R_2 respectively, and a market instrument, the underlying asset, S that is used to hedge out the market factor. The two parties default dynamics are governed by two independent point processes, J_B and J_C, which jump from 0 to 1 if a party defaults. The dynamics of these instruments are governed by the following stochastic differential equations

$$dS = \mu S dS + \sigma S dW, \tag{2.26}$$

$$dP_C = r_C P_C dt - P_C dJ_C, \tag{2.27}$$

$$dP_i = r_i P_i dt - (1 - R_i) P_i dJ_B, \quad i = 1, 2. \tag{2.28}$$

Note that subscripts for time dependency are omitted, this is done for ease of notation. Furthermore it is assumed that there is zero basis, e.g. no price difference, between the banks own bonds and thus that the relation

$$r_i - r = (1 - R_i)\lambda_B$$

holds, where r is the risk-free rate and λ_B represents the spread of a zero-recovery zero-coupon bond of the bank.

Let the total economic value of the derivative, to the bank, at time t be represented by $\hat{V}(t, S, J_B, J_C)$, then the boundary conditions at default of the bank or counterparty are

$$\hat{V}(t, S, 1, 0) = g_b(M_B, X) \quad B \text{ defaults first}, \tag{2.29}$$

$$\hat{V}(t, S, 0, 1) = g_b(M_C, X) \quad C \text{ defaults first}. \tag{2.30}$$

where $M_{B/C}$ are the general close-out amounts and X represents the collateral, which does not depend on t. For now the usual assumption about the close-out is made that that satisfies $M_B = M_C = V$, and thus

$$g_B = (V - X)^+ + R_B(V - X)^- + X, \tag{2.31}$$

$$g_C = R_C(V - X)^+ + (V - X)^- + X. \tag{2.32}$$

There are quite a few other possibilities to consider regarding the close-out amounts. For instance Burgard and Kjaer consider other possible values for $M_B = M_C$ in [BK11], while Brigo and Morini consider the cases in which $M_B \neq M_C$ [BM11].

Besides the introduction of the collateral, X, let the parameter ϕK represent the potential use, ϕ, of the capital, K, to offset funding requirements. Furthermore let I denote the initial margin posted to the counterparty. The term related to the initial margin posted to the bank is not considered, as the initial margin cannot be rehypothecated. With these parameters the following funding condition is assumed to hold

$$\hat{V} - X + I + \alpha_1 P_1 + \alpha_2 P_2 - \phi K = 0, \tag{2.33}$$

due to the fact that the bank bonds need to be used to fund or invest any excess cash and not the collateral.

Using Itô's lemma to obtain the change in value of the derivative results in the following formula

$$d\hat{V} = \frac{\partial \hat{V}}{\partial t}dt + \frac{1}{2}\sigma^2 S^2 \frac{\partial^2 \hat{V}}{\partial S^2}dt + \frac{\partial \hat{V}}{\partial S}dS + \delta\hat{V}_B dJ_B + \delta\hat{V}_C dJ_C. \tag{2.34}$$

For the semi-replicating strategy, assuming it is self-financing, the portfolio consists of Δ units of S, $\alpha_{1,2}$ and α_C units of bonds, belonging to the bank and the counterparty, cash positions, β_S, β_C, β_X, β_K and β_I, and a collateral account X. Again Itô's lemma is applied to find the change in value

$$d\Pi = \Delta dS + d\beta_S + \alpha_1 dP_1 + \alpha_2 dP_2 + \alpha_C dP_C + d\beta_C + d\beta_X + d\beta_K + d\beta_I, \tag{2.35}$$

where the dynamics of the cash accounts is governed by

$$\begin{aligned} d\beta_S &= \delta(\gamma_S - q_S)S dt, & d\beta_C &= -\alpha_C q_C P_C dt, \\ d\beta_X &= -r_X X dt, & d\beta_K &= -\gamma_K(t) K dt, \\ d\beta_I &= r_I I dt. \end{aligned}$$

The rates payed on these cash accounts are given by $(q_S - \gamma_S)$ and q_C, which represent the repo-rate and the dividend yield of the stock. By the Black and Scholes assumptions these are considered trivial, i.e. $q_{S/C} = 1$ and $\gamma_S = 0$. However for complete modelling purposes these rates are incorporated into the framework. The rates r_X and r_I are the respective rates for the collateral and initial margin. Now combining the derivative and the replicating portfolio results in

$$\begin{aligned} d\hat{V} + d\Pi = &\left[\frac{\partial \hat{V}}{\partial t}dt + \frac{1}{2}\sigma^2 S^2 \frac{\partial^2 \hat{V}}{\partial S^2} + \Delta(\gamma_S - q_S)S \right. \\ &\left. + \alpha_1 r_1 P_1 + \alpha_2 r_2 P_2 + \alpha_C r_C P_C - r_X X - \gamma_K K + r_I I \right] dt \\ &+ \epsilon_h dJ_B + \left[\Delta + \frac{\partial \hat{V}}{\partial S}\right] dS + [g_c - \hat{V} - \alpha_C P_C] dJc, \end{aligned}$$

with the hedging error on the default of the bank is given by

$$\epsilon_h = g_b - X + \alpha_1 R_1 P_1 + \alpha_2 R_2 P_2 - \phi K. \tag{2.36}$$

Using the semi-replication strategy, the value of the hedging portfolio and the derivative should satisfy the equality

$$d\hat{V} + d\Pi = 0, \tag{2.37}$$

during the derivative trade, except on the event of the default of the bank. The portfolio is exposed to the risk related to the underlying asset movements as well as the risk of the counterparty defaulting. By choosing the hedging parameters as

$$\begin{aligned} \Delta &= -\frac{\partial \hat{V}}{\partial S}, \\ \alpha_C P_C &= g_C - \hat{V}, \end{aligned}$$

these risks are eliminated. By using the funding equation 2.33 in combination with the hedging error ϵ_h and the equality $r_i = r + (1 - R_i)\lambda_B$ the following equality is obtained

$$\alpha_1 r_1 P_1 + \alpha_2 r_c P_2 = rX - rI - (r + \lambda_B)\hat{V} - \lambda_B(\epsilon_h - g_B) + r\phi K. \tag{2.38}$$

Plugging the parameter choices and equation 2.38 into equation 2.37 the partial differential equation

$$\begin{aligned} 0 =& \frac{\partial \hat{V}}{\partial t} + \frac{1}{2}\sigma^2 S^2 \frac{\partial^2 \hat{V}}{\partial S^2} - (\gamma_S - q_S) S \frac{\partial \hat{V}}{\partial S} - (r - \lambda_B - \lambda_C)\hat{V} \\ &+ g_C\lambda_C + g_B\lambda_B - \epsilon\lambda_B - s_X X - \gamma_K K + r\phi K + s_I I. \end{aligned} \tag{2.39}$$

is obtained with boundary condition $\hat{V}(T, S) = h(S)$. Note that $s_{X/I}$ represents the collateral and initial margin spread.

Note that the value of the default risky derivative portfolio, $\hat{V}$, can be written as a combination of the risk-free derivative value, V, and the risk value adjustments, U. This result in the equation $\hat{V} = V + U$, which can be plugged into equation 2.39 to obtain

$$\begin{aligned} 0 =& \frac{\partial V}{\partial t} + \frac{1}{2}\sigma^2 S^2 \frac{\partial^2 V}{\partial S^2} - (\gamma_S - q_S) S \frac{\partial V}{\partial S} - (r - \lambda_B - \lambda_C)V \\ & \frac{\partial U}{\partial t} + \frac{1}{2}\sigma^2 S^2 \frac{\partial^2 U}{\partial S^2} - (\gamma_S - q_S) S \frac{\partial U}{\partial S} - (r - \lambda_B - \lambda_C)U \\ &+ g_C\lambda_C + g_B\lambda_B - \epsilon\lambda_B - s_X X - \gamma_K K + r\phi K + s_I I. \end{aligned} \tag{2.40}$$

Now use that the risk-free derivative price satisfies the Black and Scholes Equation 2.8. Subsequently almost all terms related to V drop out and the following equation is obtained

$$\begin{aligned} 0 =& \frac{\partial U}{\partial t} + \frac{1}{2}\sigma^2 S^2 \frac{\partial^2 U}{\partial S^2} - (\gamma_S - q_S) S \frac{\partial U}{\partial S} - (r - \lambda_B - \lambda_C)U \\ &+ (g_C - V)\lambda_C + (g_B - V)\lambda_B - \epsilon\lambda_B - s_X X - \gamma_K K + r\phi K + s_I I. \end{aligned} \tag{2.41}$$

With the boundary condition given by $U(T, S) = 0$. Applying the Feynman-Kac theorem to this partial differential equation results in the expression

$$U = CVA + DVA + FCA + COLVA + KVA + MVA \tag{2.42}$$

Theorem 2.3.1 – FEYNMAN-KAC THEOREM. *Let $\mathbf{X}_t = (X_t^1, ..., X_t^d)$ be an Itô process as defined by*

$$d\mathbf{X}_t = \boldsymbol{\mu}(t, \mathbf{X}_t)dt + \boldsymbol{\sigma}(t, \mathbf{X}_t)dW_t^{\mathbb{Q}},$$

with $\boldsymbol{\mu} \in \mathbb{R}^d$, $\boldsymbol{\sigma} \in \mathbb{R}^{d\times m}$ and $W_t^{\mathbb{Q}}$ an m-dimensional $\mathbb{Q}$-Brownian motion. Define operator $\mathcal{A}_t$ by

$$A_t := \frac{1}{2}\sum_{i=1}^{d}\sum_{j=1}^{d}(\boldsymbol{\sigma}\boldsymbol{\sigma}^T)_{ij}\frac{\partial}{\partial X_t^i X_t^j} + \sum_{i=1}^{d}\mu_i(t, \mathbf{X}_t)\frac{\partial}{\partial X_t^i}.$$

Then the partial differential equation

$$\frac{\partial u}{\partial t} + \mathcal{A}_t u(t, \boldsymbol{X}_t) - r(t, \boldsymbol{X}_t)u(t, \boldsymbol{X}_t) = 0,$$

with boundary condition $u(T, \boldsymbol{X}_T)$ has solution

$$u(t, \boldsymbol{X}_t) = \mathbb{E}^{\mathbb{Q}}\left[e^{-\int_t^T r(s, \boldsymbol{X}_s)ds}u(T, \boldsymbol{X}_T)\middle|\mathcal{F}_t\right].$$

For this thesis the case of regular close-out with the semi-replication strategy as in [BK13] are considered. Therefore the following expressions for the valuation adjustments are obtained.

$$CVA = -(1 - R_C) \int_t^T \lambda_C(u) e^{-\int_t^u (r(s)+\lambda_B(s)+\lambda_C(s))ds} \mathbb{E}_t[(V(u))^+] du, \tag{2.43}$$

$$DVA = -(1 - R_B) \int_t^T \lambda_B(u) e^{-\int_t^u (r(s)+\lambda_B(s)+\lambda_C(s))ds} \mathbb{E}_t[(V(u))^-] du, \tag{2.44}$$

$$FCA = -(1 - R_B) \int_t^T \lambda_B(u) e^{-\int_t^u (r(s)+\lambda_B(s)+\lambda_C(s))ds} \mathbb{E}_t[(V(u))^+] du, \tag{2.45}$$

$$COLVA = -\int -t^T e^{-\int_t^u (r(s)+\lambda_B(s)+\lambda_C(s))ds} \mathbb{E}_t[X(u)] du, \tag{2.46}$$

$$KVA = -\int_t^T (\gamma_K(u) - r_B(u)\phi) e^{-\int_t^u (r(s)+\lambda_B(s)+\lambda_C(s))ds} \mathbb{E}_t[K(u)] du, \tag{2.47}$$

$$MVA = -\int_t^T ((1 - R_B)\lambda_B(u) - s_I(u)) e^{-\int_t^u (r(s)+\lambda_B(s)+\lambda_C(s))ds} \mathbb{E}_t[I(u)] du. \tag{2.48}$$

These terms express the KVA term in the form of an integral over the expected capital and initial margin profile respectively.

2.4 Conclusion

In the previous sections a mathematical model was defined for the pricing of derivatives under counterparty credit risk and their value adjustments. In the framework the functions for the capital and initial margin terms are not yet defined and it remains general with respect to the derivative.

To define the function for the capital term in the KVA expression choices have to be made. Because most financial institutions have regulatory requirements to hold capital related to market risk, counterparty credit risk, CVA capital, and leverage ratio capital for their over-the-counter derivatives. There are therefore several different approaches to the calculation of the required regulatory capital. In this thesis the focus lies on the counterparty credit risk part of the regulatory capital, as computed by the internal model method.

Since the nested Monte Carlo technique is very computationally heavy and is not feasible for the scope of this thesis, the next chapter is dedicated to the description of the SGBM techniques and the validation of this method will be done with the much faster Least Squares Monte Carlo method as a benchmark.

III

Capital value adjustment

In this chapter the origin of the regulatory capital requirements is described by a short synopsis of the Basel III regulatory framework related to these requirements. To quantify the regulatory capital needed for the duration of the derivative trade a set of definitions is given. Terms as loss given default, exposure at default and probability of default are defined here. Furthermore the calculations related to the regulatory capital are detailed for several approaches.

3.1 Introduction

The collapse of the financial market in 2007 instigated the idea to design regulatory reforms to address the shortcomings of the past crisis, and furthermore to make the financial sector prepared for possible future crises. During the aftermath of the financial crisis the Basel Committee introduced Basel III, [BCB11], in which significant changes with respect to capital, liquidity buffers and leverage ratios were proposed. The shortcomings, of the financial sector, which were the apparent cause of the financial crisis are stated by the Basel Committee to be the following, [Wel11]:

- The main trigger was an excess of global liquidity and leverage while maintaining deficient capital of insufficient quality and meagre liquidity buffers.
- The crises was worsened by a delevaraging process, reducing the debt levels in a multitude of sectors, and interconnectedness among financial institutions that were considered too-big-to-fail, i.e. institutions that are so big and interconnected that failure would be disastrous to the economy.
- A number of factors such as, shortcomings in risk management, market transparency, compensation practices and the quality of supervision.

To address these shortcomings and achieve the goal of *"strengthening the global capital and liquidity rules with the goal of promoting a more resilient banking sector"* by *"addressing the lessons of the financial crisis"* the Basel III framework was designed. These goals, as stated in the original Basel III document, manifested into regulations a substantial improvement of the quality and quantity of capital, with a greater focus on common equity. Secondly, to create a more comprehensive coverage of risks and a higher standard of supervision, risk management and disclosure standards. In this thesis the focus lies on the

Basel III capital and risk measures that were altered, for instance with a raise in the minimum capital requirement for common equity and an additional capital conservation buffer, and failing to fulfil there requirements would result in restrictions on dividend payments imposed by the bank.

This new regulatory framework has an impact on the pricing of derivatives since there are costs which should be incorporated into the value of a derivative. This chapter elaborates on the costs related to the holding of this capital. The expected cost of holding the regulatory capital during the life time of a trade is expressed by the capital value adjustment or as XVA term, KVA. This chapter is dedicated to the origin, structure and computation of this XVA.

The framework to include these capital costs has been discussed in Chapter 2 and is used by for instance, [JKK17], as reference framework. Furthermore Jain states the importance of recognising the impact that the rising capital requirements have on the derivative business. Since there is not yet a unifying theory on the exact computation, charging and managing of the KVA term, this thesis follows the approach as outlined by Green, Kenyon and Dennis [GKD14].

This approach divides the construction of the KVA term into three distinct categories related to different types of risk,

$$K = K_{MR} + K_{CCR} + K_{CVA}, \tag{3.1}$$

where K_{MR}, K_{CCR} and K_{CVA} represent the market risk part, the Counterparty Credit Risk, CCR, part and the Credit Value Adjustment, CVA, part respectively. The calculations needed for these risk terms are based on the future exposure profile of the derivative trade. Usually these profiles are computed by Monte Carlo simulations. However for the KVA calculations under the IMM approach would result in nested Monte Carlo simulations. For the market risk and CVA terms this nested Monte Carlo situation can be avoided by assuming a fixed VaR window. However, a more complicated situation arises in the case of the CCR term. To calculate the corresponding CCR KVA term, an outer Monte Carlo simulation of the future capital is needed, which would ideally involve an inner Monte Carlo simulation. Then the scenarios for the computation of the CCR capital should be based on the real world measure, $\mathbb{P}$, while the risk-neutral measure, $\mathbb{Q}$, should be used for the scenarios simulated to compute the expected future capital costs that need to be managed.

This thesis focuses on this problem of nested Monte Carlo simulations and how this can be avoided by the application of the LSM or the SGBM. Therefore only approaches for calculating value adjustments including this situation of nested simulations will be considered. Other approaches are not discussed as these would not benefit explicitly from the LSM and the SGBM.

3.2 Counter Party Credit Risk

For the computation of the value adjustments in this chapter, it is essential that the credit exposure of a financial derivative can be computed. This exposure can be defined as the potential loss caused by the derivative if the counter-party defaults. For most derivatives this loss is quantified by the replacements costs of the derivative. Therefore the exposure of a derivative is defined as the maximum of the derivative value V_t and zero.

Definition 3.2.1 – Exposure. *Counter party credit exposure is defined as the non-negative value of the derivatives value at time t*

$$E_t(u) := \left(\mathbb{E}^{\mathbb{Q}}\left[V_u \middle| \mathbf{S}_t\right]\right)^+.$$

Since the value of the exposure is directly linked to the value of the derivative the exposure contains a factor of uncertainty. Therefore through Monte Carlo simulations in the risk-neutral measure the distribution of the exposure can be estimated. This distribution can then be used to measure the CCR. To obtain this measure expressions are needed for the expected exposure of the underlying derivative, EE, the counterparties probability of default, PD, and the loss given default, LGD.

3.2.1 EE, PD and LGD

Given the pricing framework defined in Chapter 2, the expected exposure of a derivative at time t conditional on time u is defined by a function from the state space Ω to the positive real numbers including zero, and as stated in Basel II [BCB11], is formulated as

$$\mathrm{EE}_{(t,u)} = \mathbb{E}^{\mathbb{P}}[\mathrm{E}_t(u)] = \mathbb{E}^{\mathbb{P}}[\mathbb{E}^{\mathbb{Q}}[\mathrm{E}_u|\mathbf{S}_t]] = \int_{\Omega} \mathrm{E}_t(u,\omega)d\mathbb{P}(\omega). \tag{3.2}$$

Another essential ingredient for the quantification of CCR is the probability of default for the counter-party. There are many ways of estimating the default probability. In the scope of this thesis only a default probability that follows a constant intensity model is considered. This intensity model is described by an intensity, $\bar{h}$, and the relation

$$PD_t = 1 - e^{-\bar{h}t}. \tag{3.3}$$

The final definition needed is the loss given default, which is defined as the percentage of the exposure that the bank might loose given that a counter-party defaults. Upon default of the counter-party it is possible that the bank is able to recover a percentage of the total value of the derivative. This recovery rate is linked to the LGD through

$$LGD = 1 - \text{recovery rate}.$$

The recovery rate will be considered to be a constant throughout this thesis.

3.3 Counter-party Credit Risk capital

Before one could price the CCR capital the essential question: "what is counter-party credit risk", should be answered. Let CCR be defined as the risk that a counterparty is going into default before their financial obligations are fulfilled. This section focuses on the calculation of the capital value adjustment term related to the CCR capital, and especially on the merits of the SGBM in these calculations. The SGBM is applied in the value adjustment pricing algorithm to circumvent the need for nested simulation. Since the SGBM uses explicit expressions for the calculation of expectations it can efficiently handle the change of measure instigated by the CCR capital. The KVA calculations follow the approach as outlined in [GKD14] and [JKK17]. As in the article by Jain the methods of choice for calculating the CCR capital are the Advanced Internal Ratings-Based approach, AIRB, for the weight calculation and the Internal Model Method (IMM) for the Exposure at Default, EAD, calculation.

Consider a mathematical asset pricing framework as outlined in chapter 2. Then the inception KVA_0^{CCR} term is given by

$$\mathrm{KVA}_0^{CCR} = \mathbb{E}^{\mathbb{Q}}\left[\int_0^T p_{0,t}\gamma_t \mathrm{K}_t^{CCR} dt \middle| \mathcal{F}_0\right]. \tag{3.4}$$

Where $p_{0,t}$ is the discounting coefficient to discount the values back to time $t = 0$.

The regulatory capital that has to be held to comply with the Basel III regulations for CCR capital is defined as a capital multiplier times the risk-weighted assets, RWAs, defined as

$$\mathrm{K}_t^{CCR} = \alpha \mathrm{RWA}_t, \tag{3.5}$$

$$\mathrm{RWA}_t^{CCR} = 12.5 \times w \times \mathrm{EAD}_t, \tag{3.6}$$

where w is the weight and EAD_t is the counter-party's exposure at default, on which the following subsections elaborate.

3.3.1 Weight calculation

There are three different approaches listed in the Basel framework to calculate the weight w, such as the *Standardised Approach*, *Foundation Internal Rating-Based*, FIRB, and *Advanced Internal Rating-Based*, AIRB. Since the *Standardised Approach*, SE, simply assigns the weight based on an external rating of the counter-party and its sector it will be omitted here. The difference between FIRB and AIRB lies in the way the risk parameters are calculated. The FIRB approach and the AIRB approach are risk measurement techniques proposed under Basel II rules. The FIRB approach uses the financial institutions own empirical model for probability of default, PD, estimation, while relying on the regulators prescribed estimates for other parameters. The AIRB technique was designed to let financial institutions develop independent empirical models for the quantification required capital related to credit risk, thus allowing for more risk components than the FIRB to be estimated independently. For such internal computations, to comply the financial institution needs approval from their respective regulator. Under the AIRB approach it is thus expected that the financial institution not only estimates the PD but also the loss given default, LGD, based on quantitative models and other risk parameters. To omit this difference the FIRB and AIRB approaches will therefore be bundled into one term, IRB.

The formula for the calculation of the weight w by the IRB approach is stated by Basel II as

$$
\begin{aligned}
w &= LGD\Big(N\Big(\frac{N^{-1}(PD)}{\sqrt{1-\rho^2}} + \sqrt{\frac{\rho}{1-\rho^2}}N^{-1}(0.999)\Big)PD\Big) \times \Big(\frac{1+(M-2.5)b}{1-1.5b}\Big),\\
b &= (0.11852 - 0.05478\log(PD))^2,\\
\rho &= \left(\frac{0.24}{1-e^{-50}}\right)(1-0.5(1-e^{-50})),\\
M &= \min\left(5.0, \max\left(1.0, \frac{\sum_{t_k\leq 1} EEE_k\Delta t_k + \sum_{t_k>1} EE_k\Delta t_k}{\sum_{t_k\leq 1} EEE_k\Delta t_k}\right)\right),\\
\mathrm{EEE}_{t_k} &= \max_{t\in[0,t_k]}(EE_t),
\end{aligned}
$$

where b is a maturity adjustment, ρ the correlation coefficient, M the effective maturity and EEE_{t_k} is the effective expected exposure. These formulas are defined and enforced by the Basel Committee, due to the complexity of their derivation and lengthiness of the construction this will be omitted form this thesis, see [BCB11] for more information.

3.3.2 EAD calculation

Similar to the the weight calculation there are several different approaches to calculate the EAD_t. Initially Basel I prescribed the Current Exposure Method, CEM, for EAD estimation, however since this method is due to be replaced this method will not be discussed. Then in Basel II two new methods were proposed, the Standardised Method, SM, and the Internal Model Method, IMM. The SM was devised for financial institutions that are not qualified for internal model computation of their derivatives exposure, but need a more risk-sensitive method than the CEM. The IMM may be used after a financial institution has successfully applied to the local regulators for their permission. The IMM method is superior in the sense of risk-sensitivity and is the only method to incorporate exposure levels of future time points, [Tur10].

3.3.3 Standardised Method

In the SM, the EAD is calculated by taking the maximum of the difference between mark-to-market, MtM, value of the derivatives and the collateral compared to the difference between absolute values of the net risk positions, NRP, times the credit conversion factors, CCFs. This maximum is then multiplied by a factor β which is set to 1.4 by the regulators. The mathematical formula for the EAD is then

$$
\begin{aligned}
\mathrm{EAD}_t = \beta \times \max\Big(&\sum_i V^{(i)}_{t_{transaction}} - \sum_l V^{(l)}_{t_{collateral}},\\
&\sum_j \Big|\sum_i R^{(ij)}_{t_{transaction}} - \sum_l R^{(lj)}_{t_{collateral}}\Big| \times \mathrm{CCF}_j\Big).
\end{aligned}
$$

Where the CCFs are set by the supervisor for different types of asset classes, e.g. 0.2% for interest rate derivatives or 5% percent for gold.

3.3.4 Internal Model Method

Given the regulators permission an internal model may be used for the computation of the distribution of the future exposure. Therefore the IMM can calculate the EAD by

$$\mathrm{EAD}_t = \beta \times \mathrm{EEPE}_t, \tag{3.7}$$

where EEPE_t is the effective expected positive exposure and β is a factor that accounts for the correlation between market and credit risk, credit portfolio assumptions, concentration risk and model risk. This factor is set by the regulators to 1.4.

The weighted average over time of effective expected exposure over the first year is the EEPE_T and is calculated by taking the 1 year weighted average, by taking the integral from time t to time t plus 1 year, of the EEE_{t_k}, which is a maximum of the past expected exposure profile. This results in the formulas

$$\mathrm{EEPE}_t = \int_t^{(t+1\mathrm{year}} \max_{u\in[t,s]} \mathrm{EE}_t(u)ds, \tag{3.8}$$

$$\mathrm{EE}_t(u) = \mathbb{E}^{\mathbb{A}}[\mathrm{E}_u|\mathcal{F}_t]. \tag{3.9}$$

Where E_u is the exposure at time $u > t$. Note that the expectation in Equation 3.9 is taken under an arbitrary measure $\mathbb{A}$. By this notation it is possible to take this expectation either under the real-world, risk-neutral or a shocked measure.

3.4 Conclusion

Using the unified model presented by Green, Kenyon and Dennis [GKD14] the foundations of the valuation adjustments related to the cost of capital have been outlined, and the new " XVA" term KVA has been introduced. The multitude of different approaches to the calculation of the capital requirements, depending on regulatory permissions, illustrates the complexity of these charges and how they can differ in computational costs.

As seen from the formula-based approaches the internal model method proves to be the most complex, but also precise method of regulatory capital calculation, as it accounts very specifically for each risk component as opposed to the very general guidelines of the other methods. Therefore this thesis the main focus lies on the EAD calculations as there a change of measure occurs which will be handled by the properties of the *regress later* approach of the Stochastic Grid Bundling Method, as will be presented in the next chapter.

IV

Numerical methods

In this chapter two numerical methods for the pricing of early-exercise multidimensional derivatives are considered. These methods are described and compared by means of a multi-dimensional example problem, the pricing of a Bermuda option. The chapter starts by with the mathematical definition of the Bermudan option pricing problem. Then the numerical methods and their characteristics are elaborated on. In the final sections the methods are compared by means of test cases of the pricing problem.

4.1 Introduction

The numerical pricing of derivatives has long been a popular topic in mathematics and a lot of literature has been written about it e.g. [Hul93] or [WDH93]. In the multitude of books and articles a plethora of different approaches have been proposed such as the binomial or trinomial tree, finite difference or Monte Carlo. Each of these approaches have their own merits and limitations, be it ease of implementation, high accuracy or high generality or stability constraints.

Since the objective of this thesis is to price early-exercise derivatives and their value adjustments, it is of vital importance that only feasible methods are considered. Take for instance finite difference methods such as the Crank-Nicolson method. These methods provide both the price at inception and the hedge factor at any time t, two necessary elements for value adjustment pricing. However these finite difference methods suffer immense computational costs when they are used for highly multidimensional problems, [LS01]. Therefore finite difference methods are not considered.

To accurately price highly multidimensional derivatives the numerical methods that are considered are the least squares Monte Carlo (LSM) approach, [LS01], and the Stochastic Grid Bundling Method (SGBM), [JO15]. Both of these methods are regression-simulation based techniques combining Monte Carlo path generation with regression to determine the optimal early-exercise strategy as well as the option price.

Although both of these methods are regression based the key difference between these two is located in the local regression based on the discounted moments. The SGBM is able to approximate the continuation value more accurately than the LSM, however at some additional computational costs. Even further the SGBM uses bundles which makes the regression function simpler and can reduce the number of basis functions.

The LSM uses a *regress now* approach opposed to the *regress later* approach the SGBM employs. This means that while the LSM regression is based on discounted cash flows to approximate the expected payoff, this should only be used to calculate the optimal early-exercise time. When the approximated payoff is used for option valuation this could lead to an upward bias for the time-zero option value which arises since the maximum operator is convex, see [LS01] note 9. The SGBM does not suffer from this. Furthermore SGBM computes a *direct estimator* and a *path estimator* which, upon convergence, should differ only slightly. In the final sections of this chapter the methods are compared against each other through test-cases from the original SGBM paper, [JO15].

4.2 Bermudan option pricing

The example problem for the comparison of the numerical methods is the risk-neutral pricing of an option contract. An option contract is the agreement between two parties to trade an underlying asset at a certain time in the future, [SS06]. It can be seen as a bet on rising or falling values of the underlying asset. The two parties involved in this trade are the writer of the option and the holder. The writer creates the contract for a certain underlying asset and sells this to the holder. Then the holder has the rights granted in the option contract until the maturity time T, specified in the contract. After the maturity time the option expires and their contract becomes worthless.

These option contracts can be divided into two types, a call option and a put option. A call option lets the holder buy the underlying asset, while a put option lets the holder sell the underlying asset. This buying and selling is done at a predefined strike price K which is specified in the option contract.

Besides the buy or sell classification options can differ in the exercise possibilities. An option is exercised if the holder chooses to buy or sell the underlying for the strike. For a European option this can only be done at time T. For American options it is possible to exercise at each time $t \leq T$. Bermudan options can be exercised at a multiple of predefined times up until the expiration.

For this example problem two different dynamics for the underlying asset are considered, those defined by Black and Scholes and those of Heston.

4.2.1 The Black and Scholes model

The example problem on a d-dimensional underlying asset in a risk-neutral Black and Scholes framework as described by the previous chapter is modelled as follows. The state of the market is represented by a $\mathcal{F}_t$-adapted Itô process $\mathbf{S}_t = \{S_t^1, ..., S_t^d\}$. We consider $t \in [t_0 = 0, .., t_M = T]$ and M exercise points in time. The continuous process is thus discretized and observed at these instances t_m. Note that the number of observation times is defined here to be equal to the number of exercise times M. The dynamics of these underlying assets are given by a system of stochastic differential equations

$$\begin{aligned} dS_t^1 &= \mu_1(t, \boldsymbol{S}_t)dt + \sigma_1(t, \boldsymbol{S}_t)dW_t^1, \\ dS_t^2 &= \mu_2(t, \boldsymbol{S}_t)dt + \sigma_2(t, \boldsymbol{S}_t)dW_t^2, \\ &\vdots \\ dS_t^d &= \mu_d(t, \boldsymbol{S}_t)dt + \sigma_d(t, \boldsymbol{S}_t)dW_t^d, \end{aligned} \tag{4.1}$$

where W_t^δ are correlated Brownian motions with the correlation coefficients between W_t^i and W_t^j given by $\rho_{i,j}$ and thus let the correlation matrix be defined as

$$\boldsymbol{C} = \begin{pmatrix} 1 & \rho_{1,2} & \dots & \rho_{1,d} \\ \rho_{1,2} & 1 & \dots & \rho_{2,d} \\ \vdots & \vdots & \ddots & \vdots \\ \rho_{1,d} & \rho_{2,d} & \dots & \rho_{d,d} \end{pmatrix} \tag{4.2}$$

The adapted process $h_t = h(\mathbf{S}_t)$ represents the intrinsic value of the option. This makes the immediate payoff function of the option $\max(h_t, 0)$ at time t, thus the amount received if the holder chooses to exercise the option at time t. Now the discount factor can be calculated from the previously defined risk-free savings account process by

$$D_{t_m} := \frac{B_{t_{m-1}}}{B_{t_m}},$$

in which we consider the risk-free rate to be constant.

Now the problem can be represented as computing the maximum of the discounted expected payoff of the option contract over the time horizon

$$V_{t_0}(\mathbf{S}_{t_0}) = \max_{\tau} \mathbb{E}^{\mathbb{Q}}\left[\frac{h(\mathbf{S}_\tau)}{B_\tau}\middle|\mathbf{S}_{t_0} = \mathbf{S}\right],$$

with τ the stopping time taking values at the predefined possible exercise times and $\mathbf{S}$ the initial asset price. The value of the Bermudan option at times $t_i, i = 0...N$ is given by

$$V_{t_i}(\mathbf{S}_{t_i}) = \begin{cases} \max(h(\mathbf{S}_{t_N}, 0), & \text{for } i = N, \\ \max(h(\mathbf{S}_{t_i}), Q_{t_i}(\mathbf{S}_{t_i})), & \text{for } 1 < i < N, \\ Q_{t_i}(\mathbf{S}_{t_0}), & i = 0. \end{cases}$$

Where the conditional continuation value Q_{t_i}, the discounted expected payoff at time t_{i+1} is given by

$$Q_{t_i}(\mathbf{S}_{t_i}) = D_{t_{i+1}}\mathbb{E}^{\mathbb{Q}}[V_{t_{i+1}}(\mathbf{S}_{t_{i+1}})|\mathbf{S}_{t_i}].$$

4.2.2 The Heston model

The example problem of pricing a Bermudan option under the Heston dynamics has the same setup for the state space, exercise times and risk-free savings account process with the addition of a new state space variable: the volatility v_t. The dynamics of the underlying asset follow stochastic volatility asset dynamics defined as

$$dS_t = rS_t dt + \sqrt{v_t} S_t \left(\sqrt{1-\rho^2} dW_t^1 + \rho dW_t^2 \right),$$
$$dv_t = \kappa(\theta - v_t)dt + \gamma \sqrt{v_t} dW_t^2,$$

where $W_t^{1,2}$ are independent Brownian motions under the risk-neutral measure, κ is the mean reversion coefficient, e.g. the speed of convergence of the volatility to the long term mean, θ is the long-term mean of the volatility and γ is the volatility of the volatility parameter.

Another slight change occurs in the formula for the value of the Bermudan option since the continuation value of this option will also depend on the current state of the volatility

$$V_{t_i}(S_{t_i}, v_{t_i}) = \begin{cases} \max(h(S_{t_N}, 0), & \text{for } i = N, \\ \max(h(S_{t_i}), Q_{t_i}(S_{t_i}, v_{t_i})), & \text{for } 1 < i < N, \\ Q_{t_i}(S_{t_i}, v_{t_i}), & i = 0. \end{cases}$$

Where the conditional continuation value Q_{t_i} is given by the discounted expected payoff at time t_{i+1}:

$$Q_{t_i}(S_{t_i}, v_{t_i}) = D_{t_{i+1}} \mathbb{E}^{\mathbb{Q}}[V_{t_{i+1}}(S_{t_{i+1}}, v_{t_{i+1}})|(S_{t_i}, v_{t_i})].$$

4.3 Monte Carlo Methods

For the pricing of derivatives this thesis utilises Monte Carlo methods. Monte Carlo methods cover a broad class of algorithms that are characterised by their reliance on random sampling. This section is dedicated to the concepts of Monte Carlo methods and variance reduction techniques applied in these methods.

4.3.1 Sample path simulation

Monte Carlo methods start by generating a large number of possible future sample paths. To create these independent risk-neutral sample paths of the underlying process $\mathbf{S}_t$ different types of schemes can be used, depending on the underlying dynamics. For instance, for assets following a simple geometric Brownian motion, the Euler-Maryama scheme suffices, see Figure 4.1, will be used. For more complicated dynamics such as the Heston dynamics the more complex quadratic exponential (QE) scheme is applied, see [And08] for a detailed description.

4.4 The Stochastic Grid Bundling Method

In 2013 S. Jain and C.W. Oosterlee developed an alternative to the LSM called the Stochastic Grid Bundling Method(SGBM)[JO15]. This method is based on simulation, bundling and regression and was originally developed for the pricing of early exercise options and computing their Greeks. This was later further generalised by Feng [Fen17]. The SGBM uses a 'regress later' approach to calculate the conditional expectation instead of the

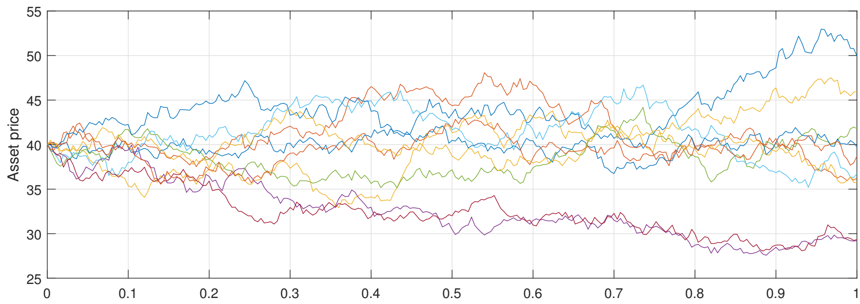

FIGURE 4.1: EXAMPLE OF 10 MONTE CARLO SAMPLE PATHS FOR AN ASSET FOLLOWING A GEOMETRIC BROWNIAN MOTION

'regress now' approach of the LSM. The section starts by illustrating the SGBM by an example problem. We begin by giving a brief description of the steps involved in the SGBM algorithm. Then the crucial parts of the SGBM algorithm are discussed individually.

- **STEP I: GRID POINT GENERATION**
  The grid point generation is done by generating N independent risk-neutral sample paths
  $$\{\mathbf{S}_{t_0}(n), ..., \mathbf{S}_{t_M}(n)\}, \text{ for } n = 1, ..., N$$
  of the underlying process $\mathbf{S}_t$. Where $\mathbf{S}_{t_m}$ represents the vector of grid points at time t_m. The starting price is given by $S_{t_0}(n) = s_0(n)$. Depending on the underlying process the appropriate discretization scheme is chosen for the generation of the sample paths, e.g. Euler-Maryama for a geometric Brownian motion or Quadratic exponential for the Heston dynamics.

- **STEP II: INITIALISATION**
  Using the the realisations of the asset values at the terminal time the terminal value of the option can be computed through
  $$V_{t_M}(\mathbf{S}_{t_M}) = \max(h(\mathbf{S}_{t_M}), 0).$$

- **STEP III: BACKWARD INDUCTION**
  While iterating backwards in time from $m = N-1, ..., 1$ the following steps are performed at each time step t_m:

  - BUNDLING
    The first step is to bundle the grid points $\mathbf{S}_m$ into ν non-overlapping sets or partitions $\mathcal{B}_m(1), ..., \mathcal{B}_m(\nu)$. This is done to approach a sample with the distribution of $\mathbf{S}_{t_{m+1}}$ conditional on the state $\mathbf{S}_{t_m}$ without simulating the conditional Monte Carlo paths.

  - THE PARAMETERIZED OPTION VALUE
    In each bundle $\beta = 1, ..., \nu$ at time t_m the values of $V_{t_{m+1}}(\mathbf{S}^{\beta}_{t_{m+1}})$ and $\mathbf{S}^{\beta}_{t_{m+1}}$ are

now given. The option values at time t_{m+1} are then approximated by ordinary least squares regression with

$$V_{t_{m+1}}(\mathbf{S}^{\beta}_{t_{m+1}}) \approx Z(\mathbf{S}^{\beta}_{t_{m+1}}, \alpha^{\beta}_{t_{m+1}}) = \sum_{k=1}^{K} \alpha^{\beta}_{t_{m+1}}(k)\varphi_k(\mathbf{S}^{\beta}_{t_{m+1}}),$$

where $\varphi_k(\cdot)$ is the k-th regression basis-function and the coefficients $\alpha^{\beta}_{t_{m-1}}$ are the regression coefficients, for these definitions see subsection 4.4.2,.

– The continuation value
With the parametrized option value $Z(\mathbf{S}^{\beta}_{t_{m+1}}, \alpha^{\beta}_{t_{m+1}})$ computed for each bundle β the continuation values of each grid point are approximated by

$$Q_{t_m}(\mathbf{S}^{\beta}_{t_m}(n)) = D_{t_m}\mathbb{E}\left[Z(\mathbf{S}^{\beta}_{t_{m+1}}, \alpha^{\beta}_{t_{m+1}})\middle|\mathbf{S}^{\beta}_{t_m} = \mathbf{S}^{\beta}_{t_m}(n)\right].$$

Which can be written as

$$\begin{aligned} Q_{t_m}(\mathbf{S}^{\beta}_{t_m}(n)) &= D_{t_m}\mathbb{E}^{\mathbb{Q}}\left[\left(\sum_{k=1}^{K} \alpha^{\beta}_{t_{m+1}}(k)\varphi_k(\mathbf{S}^{\beta}_{t_{m+1}})\right)\middle|\mathbf{S}^{\beta}_{t_m} = \mathbf{S}^{\beta}_{t_m}(n)\right], \\ &= D_{t_m}\sum_{k=1}^{K} \alpha^{\beta}_{t_{m+1}}(k)\mathbb{E}^{\mathbb{Q}}\left[\varphi_k(\mathbf{S}^{\beta}_{t_{m+1}})\middle|\mathbf{S}^{\beta}_{t_m} = \mathbf{S}^{\beta}_{t_m}(n)\right]. \end{aligned}$$

- Then given the continuation values and the early exercise policy two estimators can be computed: the direct estimator and the path estimator. A detailed description of the construction of these estimators can be found in subsection 4.4.2.

4.4.1 Bundling

For the bundling of the state space there are several techniques available and described throughout literature. One of the initial techniques proposed by Jain and Oosterlee was the *k-means* clustering technique. However this clustering algorithm runs into several problems for a high number of bundles and a highly multidimensional state space. Therefore other bundling techniques were proposed by Feng, [Fen17], and Jain and Oosterlee, [JO15].

In this section two different types of state space bundling techniques are discussed, the equal partitioning technique and the recursive bifurcation technique. Both of these techniques use a reduced state space. A mapping from the whole $N \times M \times d$ state space to a $N \times M$ reduced state space is used . This makes the bundling technique very memory efficient as opposed to storing the whole state space.

The most intuitive technique is partitioning the state space into equal partitions. The main advantage of this technique is that it guarantees that each bundle contains enough grid points to perform a regression. Which is not safeguarded for instance in the $k-means$ clustering technique.

Recursive bifurcation of the reduced state space

First the general idea behind the recursive bifurcation technique is described. As this will result in a rapid growth in bundles as the dimension increases, a reduction of the state space is introduced. This reduction technique is motivated by the stratified state aggregation method as in [BM95]. Instead of partitioning the high dimensional state space, this technique constructs a reduced state space through a mapping. To get an impression of the bifurcation algorithm Figure 4.2 illustrates an example of recursive bifurcation of the state space.

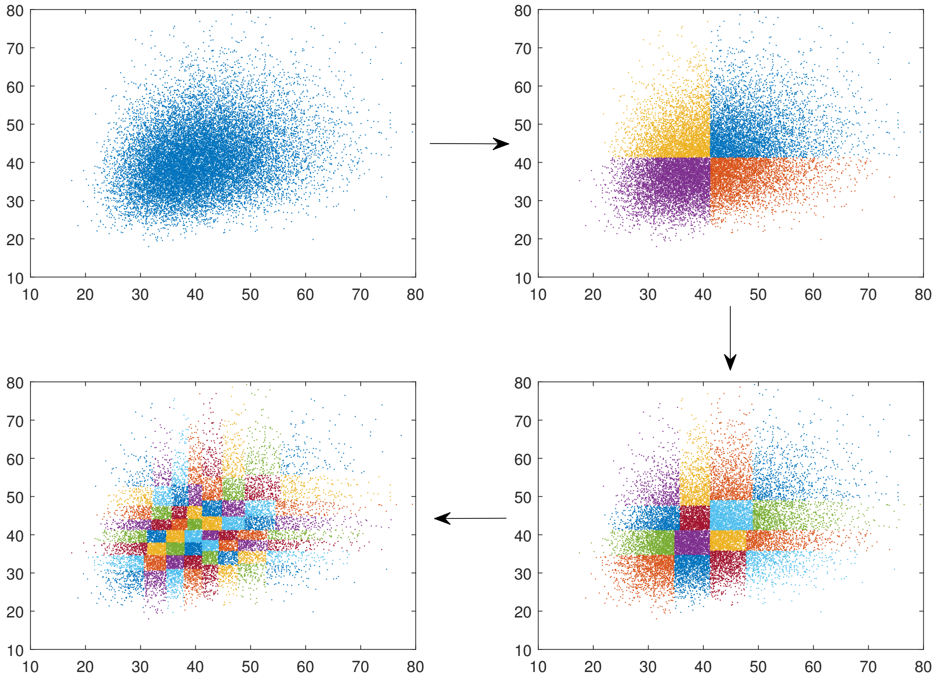

Figure 4.2: Recursive bifurcation on a two dimensional state space related to .

The reason for bundling in the SGBM is to group together grid points based on their proximity in order to obtain a simple local payoff function. A fast and practical scheme to bundle the grid points $\{\mathbf{S}_t(1), ..., \mathbf{S}_t(N)\}$ into bundles is by recursive bifurcation with the following steps:

Step I: The procedure starts by computing the mean of the set of grid points along each dimension

$$\mu_\delta = \frac{1}{N}\sum_{n=1}^{N} S_t^\delta(n), \text{ for } \delta = 1, .., d.$$

Step II: Then the grid points are divided along each dimension, $\delta = 1, ..., d$, into two disjoint subsets, one with points strictly larger than the mean, the other with points less than or equal to the dimensional mean

$$A_\delta = \{\mathbf{S}_t(n) : S_t^\delta(n) > \mu_\delta, n = 1, ..., N\},$$

$$\bar{A}_\delta = \{\mathbf{S}_t(n) : S_t^\delta(n) \leq \mu_\delta, n = 1, ..., N\},$$

Step III: From these sets the bundles will be constructed by the 2^d possible combinations of the intersections

$$\mathcal{B}(i) = \{A_1 \vee \bar{A}_1\} \cap ... \cap \{A_N \vee \bar{A}_N\}.$$

Step IV: Then perform the same steps for each bundle to split the bundles further.

This technique of bundling produces 2^d bundles in each iteration of the algorithm. Thus the number of bundles after p iterations is given by $(2^d)^p$. This can be a very fast and intuitive way of bundling the state space. However this technique becomes less attractive when the dimension of the problem increases. Since the number of bundles is directly dependent on the dimension of the state space, the number of bundles grows too rapid after each iteration.

To overcome this rapid growth of the number of bundles a reduced state spaced can be used rather than the actual state space. This reduced state space is obtained by mapping the actual state space to a lower dimensional reduced state space. For this mapping function the payoff function h is used since

$$h : \mathbb{R}^d \to \mathbb{R}$$

where $\mathbb{R}$ becomes the reduced state space with only one dimension instead of d. By then employing the recursive bifurcation bundling technique the reduced state space can be bundled. This reduces the number of bundles after p iterations from $(2^d)^p$ to 2^p.

Equal partitioning

As can be seen in Figure 4.2 the recursive bifurcation technique does not guarantee that there are enough points in each bundle to perform a feasible regression. To safeguard this assumption the reduced state space can be divided into ν partitions which contain an equal number of points.

This partitioning technique starts by reducing the multidimensional state space to a one dimensional space. Then the one dimensional data is sorted and divided over ν non-overlapping bundles. Finally the bundle indices are permuted back to the original data permutation. See Figure 4.3.

Besides the assurance of a feasible number of data points in each bundle this technique is also very usable for parallel processing. Since the dimension of the problem is decoupled of the bundling and the process does not contain iterative processes.

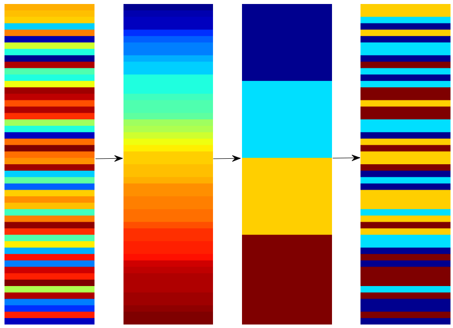

Figure 4.3: Equal partitioning technique. From left to right, start with initial one dimensional data array. The next step is to sort this array. The sorted array is bundled and in the last step re-permuted to the initial order.

Convergence of probability

To effectively use bundling to estimate the conditional expectation it is necessary that the conditional probability is conserved under bundling. Therefore the following equation should hold:

$$\lim_{\nu\to\infty}\lim_{N\to\infty}|\mathbb{P}_{N,\nu}(\mathbf{S}_{t_{m+1}}\leq y|\mathbf{S}_{t_m}=X)-\mathbb{P}(\mathbf{S}_{t_{m+1}}\leq y|\mathbf{S}_{t_m}=X)|=0, \tag{4.3}$$

where the bundled conditional probability $\mathbb{P}_{N,\nu}$ is defined as

$$\mathbb{P}_{N,\nu}(\mathbf{S}_{t_{m+1}}\leq y|\mathbf{S}_{t_m}=X):=\frac{\frac{1}{N}\sum_{n=1}^{N}\mathbf{1}_{\mathbf{S}_{t_{m+1}}(n)\leq y}(\mathbf{S}_{t_{m+1}}(n))\mathbf{1}_{\mathcal{B}_{t_m}(\beta)}(\mathbf{S}_{t_m}(n))}{\frac{1}{N}|\mathcal{B}_{t_m}(\beta)|}.$$

To satisfy this equation two assumptions are made with regard to the state space and the bundling:

Assumption I – *The set* $\mathbf{S}_{t_m}$, $m\in\{1,...,M\}$ *is an everywhere dense set of vectors valued in* $\mathbb{R}^d$, *and the probability density function of this set is continuous.*

Assumption II – *The limit of the number of paths in each bundle goes to infinity if both the paths and the number of bundles tend to infinity*

$$\lim_{\nu\to\infty}\lim_{N\to\infty}|\mathcal{B}_{t_m}(\beta)|\to\infty, m=2,...,M,\beta=1,...,\nu.$$

The proof that the absolute difference of the bundled conditional probability to the non-bundled conditional probability converges to zero under these assumptions can be found in [JO15].

4.4.2 Parameterizing of the value function

As the dimension of the state space increases the valuation function becomes more complex and could render the pricing problem intractable. Since the state space is generally large it is required to approximate the valuation function. This approximation is performed through the definition of a parameterized value function

$$Z:\mathbb{R}^d\times\mathbb{R}^K\to\mathbb{R},$$

which takes a state $\mathbf{S}_{t_m}$ and a vector α of free parameters. These free parameters are estimated through an ordinary least squares regression on a set of basis functions. However, there is first an important choice to make when constructing the parameterized value function Z. Following Jain and C.W. Oosterlee [JO15] the parameterized value function is approximated by

$$V_{t_{m+1}}(\mathbf{S}_{t_{m+1}}) \approx Z(\mathbf{S}_{t_{m+1}}, \alpha_{t_{m+1}}) = \sum_{k=1}^{K} \alpha_{t_{m+1}}(k)\varphi_k(\mathbf{S}_{t_{m+1}}).$$

Since the exact computation of the free parameter vector $\alpha^{\beta}_{t_m}$, is not feasible an approximation is used. This approximation satisfies

$$\arg\min_{\hat{\alpha}^{\beta}_{t_{m+1}}} \sum_{n=1}^{|\mathcal{B}_{t_m}(\beta)|} \left(V_{t_{m+1}}(\mathbf{S}^{\beta}_{t_{m+1}}(n)) - \sum_{k=1}^{K} \hat{\alpha}^{\beta}_{t_{m+1}}(k)\varphi_k(\mathbf{S}^{\beta}_{t_{m+1}}(n)) \right)^2,$$

and by the law of large numbers it can now be shown that under assumptions I and II the following holds

$$\lim_{N\to\infty} \left|\left| Z(\mathbf{S}_{t_{m+1}}, \hat{\alpha}_{t_{m+1}}) - Z(\mathbf{S}_{t_{m+1}}, \alpha_{t_{m+1}}) \right|\right|_{\pi} = 0,$$

with $||\cdot||_\pi$ a weighted quadratic norm.

Then the parametrized function is given by a least-squares regression. Since this type of regression gives an unbiased estimator it holds that the error of the estimation, $\eta^{\beta}_{t_{m+1}}$, expressed by

$$V_{t_{m+1}}(\mathbf{S}_{t_{m+1}}) \approx Z(\mathbf{S}_{t_{m+1}}, \hat{\alpha}_{t_{m+1}}) + \eta^{\beta}_{t_{m+1}},$$

can be neglected and thus that the following can be assumed

Assumption III – *The regression error, $\eta^{\beta}_{t_{m+1}}$, satisfies*

$$\mathbb{E}[\eta^{\beta}_{t_{m+1}}|\mathbf{S}_{t_m}(n)] = 0, \mathbf{S}_{t_m} \in \mathcal{B}_{t_m}(\beta).$$

if the number of paths in each bundle can be made sufficiently large. From this it gives that the continuation value is expressed by

$$\begin{aligned}
\hat{Q}_{t_i}(\mathbf{S}_{t_i}) &= D_{t_m}\mathbb{E}^{\mathbb{Q}}\left[V_{t_{m+1}}(\mathbf{S}_{t_{m+1}}) \middle| \mathbf{S}_{t_m} \right], \\
&= D_{t_m}\mathbb{E}^{\mathbb{Q}}\left[\sum_{k=1}^{K} \hat{\alpha}_{t_{m+1}}\varphi_k(\mathbf{S}_{t_{m+1}}) \middle| \mathbf{S}_{t_m} \right], \\
&= D_{t_m} \sum_{k=1}^{K} \hat{\alpha}_{t_{m+1}}\mathbb{E}^{\mathbb{Q}}\left[\varphi_k(\mathbf{S}_{t_{m+1}}) \middle| \mathbf{S}_{t_m} \right]. \qquad (4.4)
\end{aligned}$$

From this expression of the continuation value Theorem 4.4.1 can be derived. Which implies that the approximated continuation value converges to the analytic continuation value. Furthermore the *direct estimator* can be defined with this expression, and from that definition Theorem 4.4.2 holds under the current assumptions. Proofs of these theorems can be found in [JO15].

Theorem 4.4.1 – Convergence of the continuation approximation. *Given that assumptions* I *and* II *hold then,*

$$\lim_{\nu\to\infty}\lim_{N\to\infty}|\hat{Q}_{t_m}(\mathbf{S}_{t_m})-Q_{t_m}(\mathbf{S}_{t_m})|=0.$$

Definition 4.4.1 – Direct estimator. *The direct estimator is the value of the derivative at time t_m given by*

$$\hat{V}_{t_m}(\mathbf{S}_{t_m}(n)=max(h(\mathbf{S}_{t_m}),\hat{Q}_{t_m}(\mathbf{S}_{t_m})),n=1,...N.$$

Theorem 4.4.2 – Direct estimator bias. *Given that $\mathbb{E}[\varphi_k(\mathbf{S}_{t_{m+1}})|\mathbf{S}_{t_m}=X]$ is know exactly, and assumption* III *holds , then the direct estimator is biased high i.e.*

$$\mathbf{E}[\hat{V}_{t_0}(\mathbf{S}_{t_0}]\geq V_{t_0}(\mathbf{S}_{t_0}).$$

Corollary 4.4.1 – Direct estimator convergence. *Given that assumptions* I, II *and* III *hold then it holds that*

$$\lim_{\nu\to\infty}\lim_{N\to\infty}|\hat{V}_{t_0}(\mathbf{S}_{t_0})-Q_{t_0}(\mathbf{S}_{t_0})|=0.$$

From these theorems the important Corollary 4.4.1 follows which enables the pricing of derivatives through use of the SGBM algorithm. To obtain the direct estimation it is necessary to compute the conditional expectation, for which the characteristic function must be known in closed form.

4.4.3 Path estimator

For the calculation of the path estimator a new set of of N_L independent risk-neutral sample paths are generated, utilising the same discretisation scheme as used for the generation of the direct estimator sample paths. Then for each sample path the optimal early-exercise policy is approximated by

$$\hat{\tau}^*(\mathbf{S}(n))=min\{\mathbf{S}_{t_m}(n))\geq\hat{Q}_{t_m}(\mathbf{S}_{t_m}(n)),m=1,...,M\},$$

for which $\hat{Q}_{t_m}$ is calculated by Equation 4.4. Now the path estimator can be defined by

$$v(n)=h(\mathbf{S}_{\hat{\tau}^*(\mathbf{S}(n))}).$$

With the definition of the path estimator, Theorem 4.4.3 can be formulated. For which the proof of the bias and the convergence of the path estimator, given that Equation 4.3 holds, can be found in [BG$^+$04] as the proofs of Theorems 3 and 4, page 9.

Theorem 4.4.3 – Path estimator bias. *A low-biased estimate,$\underline{V}_{t_0}(\mathbf{S}_{t_0})$, to the true derivative value, $V_{t_0}(\mathbf{S}_{t_0})$, can be computed as:*

$$\begin{aligned}\underline{V}_{t_0}(\mathbf{S}_{t_0})&=\lim_{N_L}\frac{1}{N_L}\sum_{n=1}^{N_L}v(n),\\&\leq V_{t_0}(\mathbf{S}_{t_0}).\end{aligned}$$

4.4.4 Characteristic function

As seen in the previous sections, it is essential for the *regress later* type algorithm to be able to compute the conditional expectation expressed in basis functions as

$$\sum_{k=1}^{K} \alpha_{t_{m+1}}(k)\mathbb{E}^{\mathbb{Q}}\left[\varphi_k(\mathbf{S}_{t_{m+1}})\middle|\mathbf{S}_{t_m}=\mathbf{S}_{t_m}\right].$$

In this expression the conditional expectation can be calculated by computing the moments of the basis functions. These moments are obtained by partially differentiating the characteristic function of the basis functions.

Definition 4.4.2 – Characteristic function and moments. *The characteristic function of a random variable* $\mathbf{S}_{t_{m+1}}$ *given* $\mathbf{S}_{t_m}$ *is defined as*

$$\phi_{\mathbf{S}_{t_m}}(u_1,.,u_d|\mathbf{S}_{t_m})=\mathbb{E}\left[e^{\sum_{j=1}^{d} iu_j\mathbf{S}^j_{t_{m+1}}}\middle|\mathbf{S}_{t_m}\right].$$

Where the relation to the moments is given by

$$\mathbb{E}[(S^1_{t_{m+1}})^{p_1}...(S^d_{t_{m+1}})^{p_d}|\mathbf{S}_{t_m}]=(-i)^{p_1+...+p_d}\left[\frac{\partial^{p_1+...+p_d}\phi_{\mathbf{S}_{t_{m+1}}}(\mathbf{u})}{\partial u_1^{p_1}...\partial u_d^{p_d}}\right]_{\mathbf{u}=\mathbf{0}}. \tag{4.5}$$

Depending on the choice of basis functions, the moments can be either computed in closed form or by numerical differentiation. Since the choice of basis functions depends on the type of derivative and underlying model the characteristic function to obtain the moments is provided for each individual case. Equation 4.5 is also suitable for discretized characteristic functions. However, since those characteristic functions are approximations, the moment formula will be less accurate than an analytic expression. To overcome this drawback the number of bundles and time steps should be drastically increased which would require a GPU implementation of the SGBM algorithm. In Appendix A explicit derivations can be found for the characteristic functions used in the numerical computations performed later in this thesis.

4.5 The Least Squares Method

First published in 2001 by Longstaff and Schwartz, [LS01], the least squares Monte Carlo (LSM) approach presented a simple and powerful tool for the approximation of the prices of highly multidimensional derivatives through Monte Carlo simulation. The LSM is especially useful in the context of Bermudan and American-style exercise derivatives since this method was developed as an alternative to the existing finite difference and binomial approaches, which, as previously mentioned, perform poorly in the highly multidimensional cases of early excerise derivatives.

Although there is quite some overlap between the LSM and SGBM, the key difference between these two methods is that the LSM uses a *regress now* approach to calculate the continuation value of the derivative. This approach makes the algorithm more intuitive and computationally less complex that the SGBM. However this approach also makes the approximation of the continuation value less accurate. Furthermore the LSM does not bundle the grid points into disjoint bundles but selects the regression grid points by in-the-moneyness, which means that the payoff of the derivative should be greater than zero at that time point.

In this section an overview of the LSM algorithm is given and key aspects of the method are described in detail. Since there is much overlap with the SGBM, the LSM algorithm is only shortly discussed.

- STEP I: GRID POINT GENERATION
  Generate the grid points through various types of discretization schemes as for the SGBM.

- STEP II: INITIALISATION
  Using the realisations of the asset values at the terminal time, the terminal value can be computed through
  $$V_{t_M}(\mathbf{S}_{t_M}) = \max(h(\mathbf{S}_{t_M}), 0).$$

- STEP III: BACKWARD INDUCTION
  While iterating backwards in time from $m = N - 1, ..., 1$ the following steps are performed at each time step t_m:

  - IN-THE-MONEY PATH SELECTION
    Select all in-the-money paths $\mathcal{B} = \{n \in [1, N] | h(\mathbf{S}_{t_m}(n)) > 0\}$, thus are in-the-money.
  - CONSTRUCT THE BASIS FUNCTIONS
    Depending on the choice of $\varphi^k(\mathbf{S}_{t_m})$ the basis functions are constructed from the in-the-money paths. Then the regression is performed by
    $$\arg\min_{\hat{\alpha}_{t_m}} \sum_{n=1}^{|\mathcal{B}|} \left(V_{t_{m+1}}(\mathbf{S}_{t_{m+1}}(n)) - \sum_{k=1}^{K} \hat{\alpha}_{t_m}(k)\varphi_k(\mathbf{S}_{t_m}(n)) \right)^2$$
  - THE CONTINUATION VALUE
    Since the method uses the *regress now* approach the continuation value of the derivative can now be easily computed by
    $$\begin{aligned} Q_{t_m}(\mathbf{S}_{t_m}(n)) &= D_{t_m} \sum_{k=1}^{K} \alpha_{t_m}(k) \mathbb{E}^{\mathbb{Q}} \left[\varphi_k(\mathbf{S}_{t_m}) \middle| \mathbf{S}_{t_m} = \mathbf{S}_{t_m}(n) \right] \\ &= D_{t_m} \sum_{k=1}^{K} \alpha_{t_m}(k) \varphi_k(\mathbf{S}_{t_m}) \end{aligned}$$
  - EXERCISE POLICY
    Once the continuation value is approximated the exercise policy can be determined and the cash flows are calculated for each time step. And the value of the derivative at time t_m is given by
    $$\hat{V}(\mathbf{S}_{t_m}) = max(h(\mathbf{S}_{t_m}, Q(\mathbf{S}_{t_m})).$$

- STEP IV: PATH ESTIMATOR
  To obtain a biased low estimator for the derivative value the path estimator is calculated by
  $$V_{t_0}(\mathbf{S}_{t_0}) \geq \hat{V}_{t_0}(\mathbf{S}_{t_0}) = \frac{1}{N} \sum_{n=1}^{N} Q(\mathbf{S}_{t_1}(n)). \tag{4.6}$$
  The proof of this is statement can be found in the appendix of [LS01].

4.6 Numerical results for Bermudan option pricing

This section discusses the performance of the implementations of the SGBM and the LSM by means of numerical examples. Starting with an analysis of the different types of bundling schemes for the SGBM. Then the parameter values for the number of basis functions and Monte Carlo paths of both the SGBM and LSM are determined such that the algorithms converges sufficiently. With these parameter values a comparison between the two algorithms can be made.

The example problems on which the algorithms are tested are of increasing complexity. The first test case is a simple Bermudan put on a single asset, governed by a geometric Brownian motion, see chapter 2. This is then extended to multidimensional options, governed by correlated geometric Brownian motions, for different types of payoff functions. For the SGBM the characteristic functions and moment derivations are described in more detail in Appendix A. The four different types of options that are tested are described below.

For these tests different sets of parameters for the Bermudan option pricing dynamics are described below. To distinguish between the number of exercise times and time steps the different parameters M and Q are used respectively. Each set uses different strikes to generate in-, at- and out of the money scenario's.

<u>Set I:</u>
S_{t_0} = 40, K = {35, 40, 45}, r = 0.06, σ = 0.2, T = 1, M = 50, Q = 50.

<u>Set II:</u>
S_{t_0} = 100, K = 100, r = 0.04, T = 1, κ = 1.15, γ = 0.39, θ = 0.0348, v_0 = 0.0348, $\rho = -0.64$, M = 20.

<u>Set III:</u>
$S^{\delta}_{t_0}$ = 40, K = {35, 40, 45}, r = 0.06, σ = 0.2, ρ_{ij} = 0.25, T = 1, M = 10, Q = 10.

- I: BERMUDAN PUT OPTION ON A BLACK AND SCHOLES ASSET
  The first numerical example problem is a Bermudan put option on a single underlying asset. The dynamics of the asset price are governed by a geometric Brownian motion and the parameter set I is used. The basis functions are defined as

$$\varphi_k(S_{t_m}) = S_{t_m}^{k-1}, k = 1, ..., 5.$$

  Therefore the continuation value for the SGBM algorithm is computed by

$$\mathbb{E}[\varphi_k(S_{t_m})|S_{t_{m-1}}] = \mathbb{E}[(S_{t_m})^{k-1}|S_{t_{m-1}}],$$

  from which the moments can be calculated by

$$\mathbb{E}[(S_{t_m})^k|S_{t_{m-1}}(n)] = \left(S_{t_{m-1}}(n)e^{(r+\frac{(k-1)\sigma^2}{2})(t_m-t_{m-1})}\right)^k.$$

  As a benchmark result for the SGBM and LSM algorithms an already available COS algorithm, a method based on the Fourier cosine series expansion, reference value is used, as described in [Fen17].

- II: BERMUDAN PUT OPTION ON A HESTON ASSET
  The second numerical example problem is a Bermudan put option on a single underlying asset. In contrast to the first example the dynamics of this asset are governed by the Heston dynamics and the parameter set II is used.

  For this example the basis functions that are used are similar to that of the previous example, only the asset prices are transformed to log-asset prices, $x_{t_m} = \log(S_{t_m})$.

$$\varphi_k(x_{t_m}) = x_{t_m}^{k-1}, k = 1, ..., 5.$$

  Note that for option pricing under Heston dynamics it is also possible to incorporate the volatility state as a regression basis function, see [Fen17]. Since the SGBM showed to price with sufficient accuracy by using only state space basis functions this is omitted from this thesis.

  Then the continuation value is computed by evaluating

$$\mathbb{E}[\varphi_k(\mathbf{X}_{t_m})|\mathbf{X}_{t_{m-1}}] = \mathbb{E}[(\mathbf{X}_{t_m})^{k-1}|\mathbf{X}_{t_{m-1}}],$$

  where $\mathbf{X}_{t_m} = \{x_{t_m}, v_{t_m}\}$. The derivation of the explicit formula for these moments from the characteristic function is given in Appendix A.

- III: BERMUDAN GEOMETRIC BASKET PUT OPTION ON MULTIPLE ASSETS
  The third numerical example problem is a Bermudan put option on the geometric average of multiple assets. The dynamics of the underlying asset prices are governed by correlated geometric Brownian motions and the parameter set III is used.

  The payoff function of this basket option is the strike price minus the geometric average of the d assets,

$$h(\mathbf{S}_{t_m}) = K - (\prod_{\delta=1}^{d} S_{t_m}^{\delta})^{\frac{1}{d}}.$$

From this payoff function follows the choice of basis functions as

$$\varphi_k(\mathbf{S}_{t_m}) = \Big((\prod_{\delta=1}^{d} S^{\delta}_{t_m})^{\frac{1}{d}} \Big)^{k-1}.$$

The continuation value can now be computed by

$$\mathbb{E}[\varphi_k(\mathbf{S}_{t_m})|\mathbf{S}_{t_{m-1}}] = \mathbb{E}[(\prod_{\delta=1}^{d} S^{\delta}_{t_m})^{\frac{k-1}{d}}|\mathbf{S}_{t_{m-1}}],$$

from which the moments can be calculated by

$$\mathbb{E}[\varphi_k(\mathbf{S}_{t_m})|\mathbf{S}_{t_{m-1}}S(n)] = \Big(P_{t_{m-1}} e^{(\bar{\mu}+\frac{(k-1)\bar{\sigma}^2}{2})\Delta t} \Big)^{k-1}.$$

Where,

$$P_{t_{m-1}}(n) = \Big(\prod_{\delta=1}^{d} S^{\delta}_{t_{m-1}} \Big)^{\frac{k-1}{d}}, \bar{\mu} = \frac{1}{d}\sum_{\delta=1}^{d}(r - \frac{\sigma^2_{\delta}}{2}), \bar{\sigma}^2 = \frac{1}{d^2}\sum_{i=1}^{d}\sum_{j=1}^{d} \rho_{i,j}\sigma_i\sigma_j$$

- III: Bermudan arithmetic basket put option on multiple assets
  The fourth numerical example problem is a Bermudan put option on the arithmetic average of multiple assets. The dynamics of the underlying asset prices are governed by correlated geometric Brownian motions and the parameter set III is used.

  The payoff function of this basket option is the strike price minus the arithmetic average of the d assets,

$$h(\mathbf{S}_{t_m}) = K - \frac{1}{d}\Big(\sum_{\delta=1}^{d} S^{\delta}_{t_m} \Big).$$

  From this payoff function follows the choice of basis functions as

$$\varphi_k(\mathbf{S}_{t_m}) = \Big(\frac{1}{d}(\sum_{\delta=1}^{d} S^{\delta}_{t_m}) \Big)^{k-1}, k = 1, ..., 3.$$

  The continuation value can now be computed by

$$\mathbb{E}[\varphi(\mathbf{S}_{t_m})|\mathbf{S}_{t_{m-1}}] = \mathbb{E}[(\frac{1}{d}\sum_{\delta=1}^{d} S^{\delta}_{t_m})|\mathbf{S}_{t_{m-1}}].$$

  This expectation can be computed by rewriting it as a linear combination of moments of the geometric average of assets. This is then expressed as

$$\Big(\sum_{\delta=1}^{d} S^{\delta}_{t_m} \Big)^{k} = \sum_{k_1+k_2+...+k_d=k} \binom{k}{k_1, k_2, ..., k_d} \prod_{1\le\delta\le d} (S^{\delta}_{t_m})^{k_\delta}.$$

4.6.1 Experiments with the bundling of the SGBM algorithm

To use the SGBM algorithm as numerical method for the pricing of derivatives, it is essential that parameters are used that can guarantee a certain degree of convergence. Since the bundling of the state space is one of the essential steps in the algorithm, this section analysis which bundling technique should be used. In the previous section two different types of state space bundling techniques are discussed, recursive bifurcation and equal partitioning. The performance of these two techniques are compared. As can be seen from Table 4.1 and Figure 4.4, the two proposed methods of bundling do not differ significantly in accuracy. For $\nu = 16$ bundles all the algorithms valuations are within one standard deviation of the true prices.

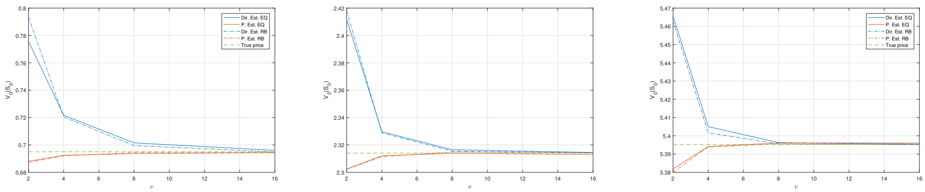

(a) Out of the money $K = 35$ (b) At the money $K = 40$ (c) In the money $K = 45$

Figure 4.4: The results for both types of bundling in the SGBM algorithm. The algorithm is applied to a Bermudan put option for three different types of strikes.

Strike	*Bundling*	*Estimator*	$\nu = 2$	$\nu = 4$	$\nu = 8$	$\nu = 16$
35	RB	*direct*	0.7933 (0.0007)	0.7207 (0.0013)	0.6997 (0.0003)	0.6949 (0.0002)
		path	0.6874 (0.0026)	0.6919 (0.0029)	0.6933 (0.0024)	0.6941 (0.0020)
	EP	*direct*	0.7756 (0.0006)	0.7216 (0.0010)	0.7015 (0.0004)	0.6960 (0.0002)
		path	0.6881 (0.0018)	0.6924 (0.0032)	0.6937 (0.0025)	0.6943 (0.0028)
40	RB	*direct*	2.4167 (0.0020)	2.3289 (0.0004)	2.3155 (0.0001)	2.3142 (0.0001)
		path	2.3013 (0.0040)	2.3130 (0.0030)	2.3140 (0.0021)	2.3134 (0.0020)
	EP	*direct*	2.4126 (0.0020)	2.3297 (0.0005)	2.3165 (0.0001)	2.3141 (0.0001)
		path	2.3010 (0.0042)	2.3120 (0.0037)	2.3127 (0.0034)	2.3134 (0.0035)
45	RB	*direct*	5.4625 (0.0009)	5.4016 (0.0003)	5.3956 (0.0001)	5.3953 (0.0001)
		path	5.3793 (0.0042)	5.3937 (0.0037)	5.3960 (0.0035)	5.3961 (0.0042)
	EP	*direct*	5.4628 (0.0018)	5.4016 (0.0005)	5.3956 (0.0001)	5.3953 (0.0001)
		path	5.3800 (0.0034)	5.3939 (0.0045)	5.3955 (0.0040)	5.3952 (0.0035)

Table 4.1: Convergence of the SGBM algorithm for increased number of bundles. The reference values for this Bermudan put options are $V_0 = 0.6940$, $V_0 = 2.3140$ and $V_0 = 5.3952$.

Another way to make a comparison between the two bundling techniques is to analyse the impact of the different bundling on the computation time. In Figure 4.5 the computation time for the bundling techniques is illustrated. The two techniques are each performed 30 times on the same set of random numbers for an increasing number of bundles. The equal partitioning bundling technique clearly outperforms the recursive bifurcation technique, being up to 30 times faster for $\nu = 1024$.

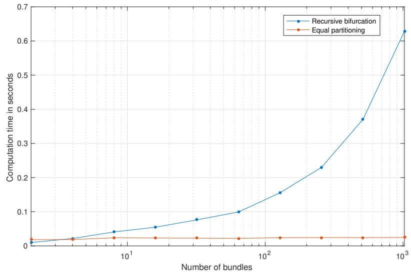

ν	RB	EP
2	0.0097	0.0183
4	0.0217	0.0186
8	0.0408	0.0237
16	0.0548	0.0231
32	0.0763	0.0228
64	0.0993	0.0221
128	0.1555	0.0239
256	0.2299	0.0245
512	0.3704	0.0242
1024	0.6286	0.0247

Figure 4.5: A comparative plot of the computation times for the RB and EQ bundling techniques on an array of 2×10^5 random asset values into ν bundles.

From the results of the convergence and computation time tests, it seems that two bundling techniques perform almost similar in accuracy. Computationally however, the equal partitioning technique has significantly lower costs. Furthermore, an important aspect of the equal partitioning bundling technique is that it safeguards the condition that there is a sufficient number of grid points present in each bundle. Therefore the equal partitioning technique is favoured in this thesis to avoid under filled bundles, and will thus be used for further test with the SGBM algorithm.

For the example problem of the Bermudan put option on a Heston asset the state space can be bundled in two dimensions, both for the log-asset value and the volatility. To verify if the equal partitioning bundling technique also suffices for this type of bundling a convergence test is performed. The parameters used in this set are those of Set II. The set of parameters is chosen in such a way that the Feller condition, $2\kappa\theta > \gamma$, is not satisfied and thus that v_t can become negative. This means that the volatility process can become zero and numerical methods may suffer from this.

The results in Figure 4.6 illustrate the convergence of the SGBM for an increasing number of basis functions. It is shown that an increase in basis functions increases the accuracy of the SGBM. However if the number of bundles is increased sufficiently the SGBM can employ a lower order of basis functions for the same accuracy. A side note should be made that the logarithm in the characteristic function is in many software packages restricted to its principle branch. However in this thesis, using the same argument as Ruijter and Oosterlee, [RO12], since the results converge to the correct price for the tested parameter set this will not be discussed in more detail.

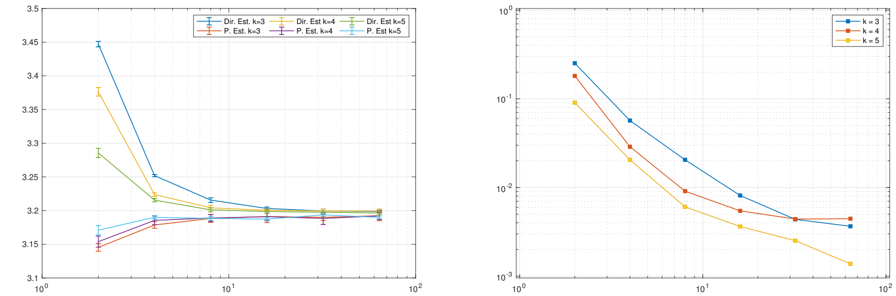

(A) (B)

Figure 4.6: (A) - Bermudan option prices. (B) - Error against reference value $V_0 = 3.1950$.

To verify the SGBM convergence in higher dimensional problems, the multidimensional example cases of the geometric- and arithmetic average Bermudan put options are analysed for parameter set II. The parameters are tested for a variety of different dimensions namely, $d = 5, 10$ and 15, with $N = 5 \cdot 10^4$, $N_L = 4 \cdot N$ and the EP bundling technique. The results of the convergence test are illustrated in Figure 4.7 and it is evident that for the chosen parameter settings the convergence of the multidimensional algorithm is similar to the single dimensional convergence.

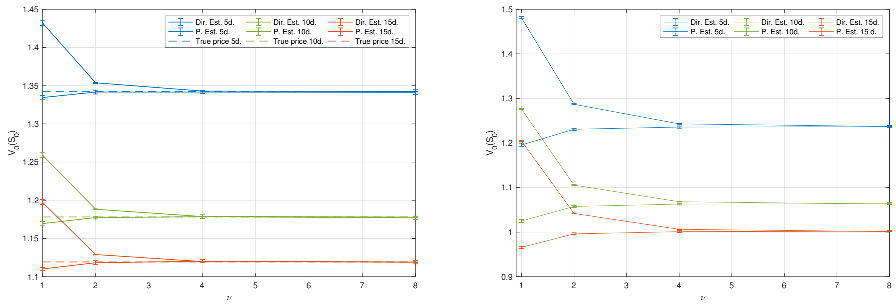

(A) (B)

Figure 4.7: (A) - Geometric average basket option. (B) - Arithmetic average basket option. (C) Comparison table.

4.6.2 Experiments with the basis functions of the LSM algorithm

Since the conditional expectation in the formula for the continuation value is deterministic, the LSM can choose from a wide variety of basis functions. The original paper, [LS01], discussing the LSM algorithm states that choices for the basis functions include Laguerre, Hermite, Legendre, and Chebyshev polynomials. These types of basis functions are illustrated in Figure 4.8.

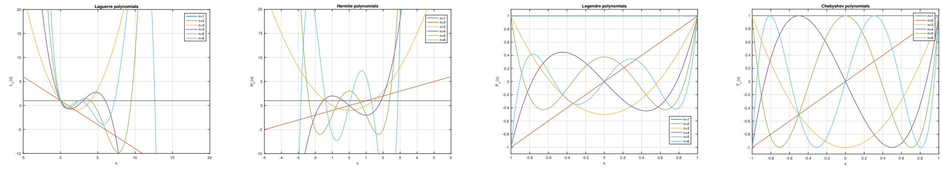

(A) LAGUERRE (B) HERMITE (C) LEGENDRE (D) CHEBYSHEV

FIGURE 4.8: THE FOUR DIFFERENT TYPES OF BASIS FUNCTIONS OF THE LSM ALGORITHM, EACH FIGURE DISPLAYS THE FUNCTIONS UP TO 6 TERMS.

To determine the number of basis functions needed to obtain accurate approximations the theoretical convergence result from Equation 4.6 is used. This equation states that by increasing the number of basis functions k the value of the LSM algorithm will increase towards the true value of the derivative. In Figure 4.9a the values of the LSM algorithm for increasing values of k, are shown for a single Bermudan put option. It is evident from this Figure that the LSM algorithm converges after $k = 3$. In Figure 4.9b it is seen that the computation time of the LSM increases steadily for higher numbers of basis functions. This implies that the LSM algorithm will not gain in accuracy for an increased computation time after $k = 3$. Therefore it is evident that this should be the preferred number of basis functions for the LSM algorithm.

The second test for convergence is done by selecting the sufficient number of basis functions and increasing the number of Monte Carlo paths such that the value of the LSM algorithm is within an arbitrary ϵ range of the true value, which implies that the LSM algorithm converges to the desired degree of accuracy, see Proposition 2 in [LS01] for the proof of this convergence. Figure 4.9c shows that the LSM algorithm indeed converges as expected for an increasing number of Monte Carlo paths. From now on $N = 10^6$ is assumed for the LSM algorithm as sufficient convergence is achieved and computational costs increase quite steeply for larger values of N.

As is displayed by the results of the two tests on the LSM algorithm the influence of the type of basis function is negligible. Therefore the type basis functions used in the LSM algorithm is chosen to be the Legendre polynomials, which are also used in the original paper [LS01].

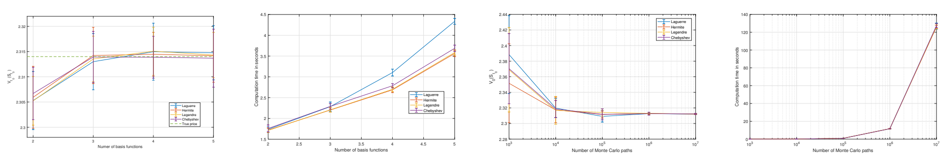

(A) (B) (C) (D)

FIGURE 4.9: (A) - CONVERGENCE FOR AN INCREASING NUMBER OF BASIS FUNCTIONS. (B) - COMPUTATION TIME FOR DIFFERENT TYPES OF BASIS FUNCTIONS. (C) - CONVERGENCE FOR AN INCREASING NUMBER OF MONTE CARLO PATHS. (D) - COMPUTATION TIME FOR AN INCREASING NUMBER OF MONTE CARLO PATHS.

4.7 SGBM compared to LSM

To test the SGBMs and LSMs performance the two methods are applied to the same example problems and then compared. The parameters for each method are the parameters found in the previous section that will provide a sufficiently converged result, which is needed to make a useful comparison.

The first test problem is the Bermudan put option on a single underlying asset. The same problem is used for the Black and Scholes and Heston dynamics. The algorithms are run for an increasing number of Monte Carlo sample paths to see the evolution of the computational time and the standard deviation. Each test is run for 30 times to obtain the average values and deviations. For the Black and Scholes test case $\nu = 16$ is used and $\nu = 64$ for the Heston case for convergenced results.

	Black and Scholes					Heston				
	SGBM			LSM		SGBM			LSM	
N	Dir. Est.	P. Est.	Time	P. Est.	Time	Dir. Est.	P. Est.	Time	P. Est	Time
10^4	2.3839 (0.0011)	2.3037 (0.0078)	1.1338	2.3057 (0.0121)	0.1049	1.1013 (0.0017)	1.1047 (0.0065)	2.5816	1.1106 (0.0190)	0.9653
$5 \cdot 10^4$	2.3838 (0.0005)	2.3046 (0.0036)	4.8947	2.3071 (0.0066)	0.5283	1.1012 (0.0007)	1.1024 (0.0036)	11.6317	1.0995 (0.0056)	6.5067
10^5	2.3838 (0.0004)	2.3064 (0.0030)	9.0859	2.3045 (0.0052)	0.9868	1.1012 (0.0005)	1.1024 (0.0020)	23.8740	1.0959 (0.0037)	13.5206
$5 \cdot 10^5$	2.3838 (0.0002)	2.3055 (0.0011)	50.1851	2.3047 (0.0020)	5.4735	1.1011 (0.0002)	1.1020 (0.0011)	116.1618	1.0946 (0.0018)	72.5676

Table 4.2: A comparison of the SGBM and LSM for the Black and Scholes and Heston models on a single underlying asset. Set I is used with $M = Q = 20$ for the BS test, and set II is used for Heston but with $v_0 = \theta = 0.055$ and $\gamma = 0.9$.

It is clear from Table 4.2 that the SGBM algorithm has a lower standard deviation in the direct estimator for roughly the same computation time, and has an increased accuracy for the same number of sample paths for the Black and Scholes model. Regarding the Heston model the the the SGBM is quite a bit slower, due to the higher number of bundles needed to obtain accurate results. However, the SGBM method is much more accurate, even given a smaller number of Monte Carlo paths.

As has been done for the SGBM algorithm the LSM algorithm is also applied to the multidimensional cases, the geometric and arithmetic average basket options. For these options the parameter settings of Set II are used. The algorithms are tested for three different multidimensional cases, $d = 5, 10$, and 15. The results of these calculations are displayed in Figure 4.7. In Figures 4.7 (A) and 4.7 (B) it is evident that the SGBM algorithm also converges for the multidimensional cases. In Table 4.3 the numerical values of the SGBM algorithm and the LSM algorithm are given and the computation times. From those numbers it can be concluded that the LSM algorithm converges for the estimated parameter values. Furthermore Table 4.3 is in line with the claim that the SGBM algorithm provides the option value with a higher precision in comparable computation time.

	Geometric					Arithmetic				
	SGBM			LSM		SGBM			LSM	
d	Dir. Est.	P. Est.	Time	P. Est.	Time	Dir. Est.	P. Est.	Time	P. Est	Time
5	1.3421 (0.0002)	1.3414 (0.0026)	5.91	1.3417 (0.0016)	7.8245	1.2364 (0.0004)	1.2364 (0.0022)	4.5765	1.2362 (0.0018)	8.3690
10	1.1779 (0.0001)	1.1780 (0.0018)	6.49	1.1779 (0.0012)	9.1105	1.0626 (0.0003)	1.0626 (0.0020)	6.8796	1.0622 (0.0008)	9.3967
15	1.1190 (0.0002)	1.1184 (0.0026)	6.81	1.1187 (0.0008)	10.5784	1.0010 (0.0003)	1.0013 (0.0018)	10.0624	1.0622 (0.0012)	9.3967

Table 4.3: A comparison of the SGBM and LSM algorithm for geometric and arithmetic basket options.

4.8 Conclusion

This chapter has introduced both the Stochastic Grid Bundling Method and the Least Squares Monte Carlo method. Through numerical examples both methods have proved to be suitable algorithms for the computation of Bermudan option prices, under the dynamics described in Chapter 2.

Arguments for the choice of state space bundling technique and basis functions related to the local regression were presented, and the convergence of the algorithms for these choices was analysed. It was shown that for the SGBM both the direct estimator and the path estimator converged, and that the LSM converged both in number of basis functions and Monte Carlo paths. The single and multidimensional numerical example cases were shown to be solvable by the algorithms with any desired degree of accuracy.

Now that the algorithms for pricing the Bermudan options are defined and proven to be working the final step of this thesis can be made, the calculation of the KVA. The next chapter is dedicated to the necessary steps for this calculation.

V

Numerical KVA

This chapter presents the cumulative of the previous chapters. The mathematical framework in which the options are priced, together with the construction of the capital regulations and the numerical methods for their computation. Furthermore a new case study is presented for the pricing of KVA for Bermudan options, which has been the primary objective of this thesis. The chapter ends with a discussion of these new results.

5.1 Introduction

In Chapter 3 general expressions for the computation of KVA have been defined. This chapter is dedicated to the numerical aspects of these KVA formulas. With the SGBM algorithm as defined in the previous chapter in place for the computation of Bermudan option prices, the first hurdle on the road to the KVA pricing is the calculation of the expected exposure. The validation of these computations is done through reference values obtained from the calculations made with the Monte Carlo COS method by Shen, [She14].

The second part is incorporating the formulas to calculate the exposure at default values, with which the need for the SGBM algorithm rises, as these calculations may involve a change of measure. With a standard Monte Carlo approach this would lead to the situation of nested Monte Carlo simulations, e.g. for each Monte Carlo path, at each time step another Monte Carlo simulation would be needed to price the outer Monte Carlo time step. This unfavourable situation, due to its computationally heavy property is subsequently circumvented by the SGBM, using the SGBM KVA algorithm presented by Jain, Karlsson and Khandai in [JKK17].

The SGBM KVA algorithm is applied to a case study of Bermudan options. For this there are several details of the algorithm which need to be altered in order to correctly price a Bermudan derivative, as opposed to the non Bermudan test cases presented in the original publication. Then, with the algorithm that is compatible with the Bermudan options, the chapter presents new case studies for each of the example problems as seen in the previous chapter, and ends with a discussion of these results.

5.2 Expected exposure

The exposure of a derivative has previously been defined as the potential loss in case of a counterparty default. However for Bermudan options the exposure is zero once the option is exercised, and otherwise equals to the continuation value:

$$\mathrm{E}_{t_m} = \begin{cases} 0, & \text{if exercised,} \\ Q_{t_m}(\mathbf{S}_{t_m}), & \text{if not exercised.} \end{cases}$$

This means that going backwards through time, the exposure of each grid point is set to their corresponding continuation value. Then the continuation values are checked against the immediate exercise values. Since a Bermudan option has the possibility to be exercised earlier than the maturity, it is important that once the immediate exercise value is greater or equal to the continuation value the option is exercised. If this event occurs, the option value becomes zero for the remainder of the time horizon. Thus the exposure values of the future times of that exercised Monte Carlo path are set to zero.

Since it is necessary to have the possibility of setting the future exposure values to zero, the exposure values are calculated for all observation times and Monte Carlo paths are stored. Then if a path is exercised the future exposure values are set to zero. Thus the average expected exposure under $\mathbb{Q}$ at time t_m can be computed after all observation times have been iterated through by taking the average of these calculated exposures.

$$\mathrm{EE}_{t_m}(t_{m+1}) = \frac{1}{N}\sum_{i=1}^{N} \mathrm{E}_{t_{m+1}}$$

The process of the $\mathrm{EE}_{t_m}(t_n)$ calculation is illustrated in Figure 5.1a for $t_m \in [0, T],\ t_n = T$, as seen from time t_0. In this Figure the exposure values of three sample paths in the Monte Carlo simulation of the price of the underlying asset are plotted by a dot for each grid point. To illustrate the distribution of the exposure values the 97.5 quantile and 2.5 quantile values for each time step are plotted by the dashed green line, the potential future exposure, PFE. The blue line represents the value of the expected exposure, the average of the exposure values at each time step.

To validate the values of the calculated expected exposure the results from a numerical test performed in [Fen17] are used as a benchmark to test the implementations of the SGBM and LSM algorithms. The numerical example problem is the pricing of a Bermudan put option for parameters: $S_{t_0} = 100$, $K = 100$, $r = 0.05$, $\sigma = 0.2$, $M = 50$ and $T = 1$. For the reference values Feng used the MC COS method to calculate the expected exposure. In Figure 5.1 B a comparison of the SGBM and MC COS values are displayed.

For the Heston dynamics the calculations of the expected exposure are similar to those of the Black and Scholes. The impact of the stochastic volatility can however be displayed by particular choices of the parameters. Since for a γ value small enough, the option price under Heston dynamics, given that the initial volatility v_0 and long term mean volatility θ are equal, should approach the Black and Scholes price. From the in Figure 5.2 displayed example tests it is clear that for smaller values of γ the Heston model converges to the Black and Scholes model. The calculations are done for parameter set II of the previous chapter, with the alterations $T = 0.25$ and $M = Q = 50$.

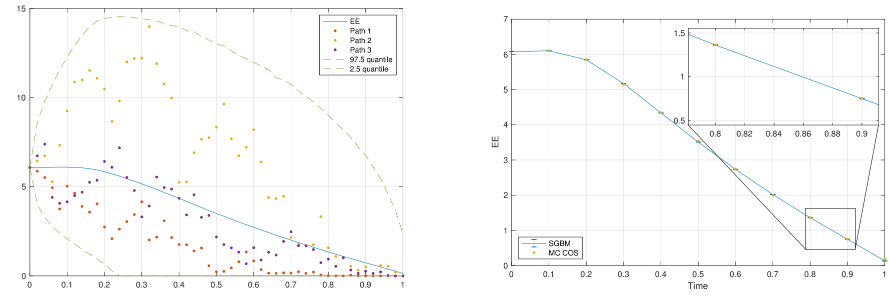

(A) (B)

Figure 5.1: (A) - Exposure values of a Bermudan option for different sample paths. (B) - A comparison in Expected exposure values of a Bermudan option for different numerical methods.

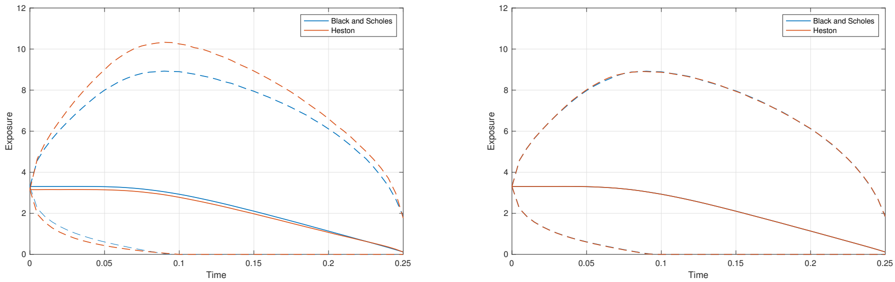

(A) (B)

Figure 5.2: (A) - A Black and Scholes option and a Heston option with $\gamma = 0.39$. (B) - A Black and Scholes option and a Heston option with $\gamma = 0.0001$.

5.3 The SGBM approach for KVA

To introduce the difference between the calculation of the KVA value for Bermudan and non Bermudan options let's first consider the non Bermudan example as used in [JKK17]. The method is started by calculating the values, V_{t_m}, of the portfolio for each time $t_0, ..., t_M$ for each of the N generated sample paths. Then for each time step the paths are bundled into ν bundles $\mathcal{B} = \beta_1, ..., \beta_\nu$. Then the conditional expectation of the future exposure value of the portfolio is calculated, using the SGBM style regression approach:

$$\begin{aligned} \mathrm{EE}_{t_m}(t_u, n) &= \mathbb{E}\left[\mathrm{E}_{t_u}\middle|\mathcal{F}_{t_m}\right], \\ &= \mathbb{E}\left[\mathbb{E}\left[\mathrm{E}_{t_u}\middle|\varphi(\mathbf{S}_{t_u}), \mathbf{S}_{t_m}(n)\right]\middle|\mathbf{S}_{t_m}(n)\right]. \end{aligned}$$

Where $\varphi(\mathbf{S})$ are the basis functions, which will be simple polynomial of the underlying in this example. This inner expectation is then approximated by

$$\mathbb{E}\left[\mathrm{E}_{t_u}\middle|\varphi(\mathbf{S}_{t_u}), \mathbf{S}_{t_m} \in \beta_b\right] = \sum_{k=1}^{K} \alpha_{t_m,t_u}^{\beta_b,k} \varphi_k(\mathbf{S}_{t_u}).$$

Where $\alpha^{\beta_b}_{t_m,t_u}$ satisfies

$$\underset{\alpha^{\beta}_{t_m,t_u}}{\arg\min} \sum_{n=1}^{|\mathcal{B}_{t_m}(\beta)|} \left(V_{t_u}(\mathbf{S}^{\beta}_{t_u}(n)) - \sum_{k=1}^{K} \alpha^{\beta,k}_{t_m,t_u}(k)\varphi_k(\mathbf{S}^{\beta}_{t_u}(n)) \right)^2. \tag{5.1}$$

Thus resulting in the following equation for the conditional expectation of the future exposure

$$\mathrm{EE}_{t_m}(t_u,n) = \alpha^{\beta_b,k}_{t_m,t_u}\mathbb{E}^{\mathbb{P}}\left[\varphi_k(\mathbf{S}_{t_u}(n)) \middle| \mathbf{S}_{t_m}(n) \in \mathcal{B}_{t_m}(\beta)\right]. \tag{5.2}$$

As these moment functions are known, see Chapter 4, the expected exposure under measure $\mathbb{P}$ can be computed without the need of nested simulations, since as the number of bundles increases and when N is sufficiently large a nested Monte Carlo effect is obtained without extra simulations. It should be noted that the assumption is made that the same underlying process drives the risk factors under both $\mathbb{Q}$ and $\mathbb{P}$.

The summerised steps of the algorithm for the SGBM KVA calculation are given in Algorithm 1 in pseudo-code.

Algorithm 1: KVA-SGBM

Generate the grid points $\mathbf{S}_{t_0},...,\mathbf{S}_{t_M}$.
Calculate the values $V_{t_m}(\mathbf{S}_{t_m})$.
for $m = 0,...,M$ **do**
  Bundle the grid points into ν bundles.
  for $b = 1,...,\nu$ **do**
    for $n = m+1,...,M$ **do**
      Compute all regression coefficients $\alpha^{b,k}_{t_m,t_n}$, Equation 5.1.
      Compute $\mathrm{EE}_{t_m}(t_n,\mathbf{S}_{t_m})$, Equation 5.2.
for $m = M,...,0$ **do**
  Compute the EEPE_{t_m} using Equation 3.8 and the $\mathrm{K}^{\mathrm{CCR}}_{t_n}$ using Equation 3.5.
Calculate the KVA_{t_0} using Equation 3.4.

5.3.1 Algorithm verification

To verify if the KVA computation algorithm implementation is working correctly and is creating accurate results, the algorithm's output as presented in [JKK17] is replicated in Figure 5.4. These results represent the computation of the KVA on a portfolio consisting of five FX forward contracts on a FX rate following a geometric Brownian motion with $r = 0.001991$, $\sigma^{\mathbb{Q}} = \{0.100875, 0.200875\}$ and $\sigma^{\mathbb{P}} = 0.100875$, with $\gamma_t = 0.2$ and $\mathrm{PD} = 0.02$. As can be seen in Figure 5.3 the current implementation of the algorithm is able to replicate the results as presented by Jain, Karlsson and Kandhai in Figure 2 of [JKK17] and can thus be subjected to the new test case.

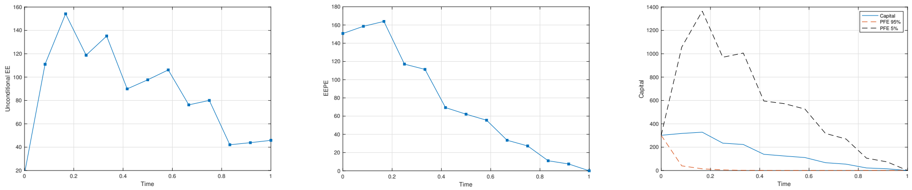

(A) (B) (C)

FIGURE 5.3: (A) - UNCONDITIONAL EXPECTED EXPOSURE VALUES (B) - EFFECTIVE EXPECTED POSITIVE EXPOSURE. (C) - REGULATORY CAPITAL WITH PFE 95% AND PFE 5%.

5.3.2 THE BERMUDAN ALGORITHM

To use the SGBM approach for the fast change of measure calculation in the problem of Bermudan option pricing a few changes have to be made. Since there are some differences in assumptions that can be made the a few key points of the algorithm should be revisited. One of these changes regards the assumption about the value of the exposure at time t_m given $\mathcal{F}_{t_m}$. In the non Bermudan FX forward contract example case used in [JKK17] the formula used for the expected exposure of the derivative at time t_m given time $\mathcal{F}_{t_m}$ is

$$\begin{aligned}\mathrm{EE}_{t_m}(t_m) &= \frac{1}{N}\sum_{i=1}^{N} \mathrm{E}^{\mathbb{P}}_{t_m}(\mathbf{S}_{t_m}(i)),\\ &= \frac{1}{N}\sum_{i=1}^{N} h(\mathbf{S}_{t_m}(i)), = V^{\mathbb{P}}_{t_m} = V_{t_m}.\end{aligned}$$

Where the last equality can be made since the value of the FX forward contract does not depend on the future values of the derivative, e.g. the continuation value. However, this is evidently not the case for Bermudan derivatives. This means that that last equality does not hold, therefore the following equation should be used, that uses the continuation value.

$$\begin{aligned}\mathrm{EE}_{t_m}(t_m) &= \frac{1}{N}\sum_{n=1}^{N} E^{\mathbb{P}}_{t_m}(t_m),\\ &= \frac{1}{N}\sum_{i=1}^{N} \begin{cases} 0 & \text{if exercised,}\\ Q^{\mathbb{P}}(\mathbf{S}_{t_m}(n)) & \text{if not exercised,}\end{cases},\\ &= \frac{1}{N}\sum_{n=1}^{N} \begin{cases} 0 & \text{if exercised,}\\ \sum_{k=1}^{K} \alpha^{\beta,k}_{t_m}\mathbb{E}^{\mathbb{P}}[\varphi_k(\mathbf{S}_{t_{m+1}}(n))|\mathbf{S}_{t_m}(n)] & \text{if not exercised,}\end{cases}\end{aligned}$$

With $\alpha^{\beta,k}_{t_m}$ the regression coefficients satisfying

$$\underset{\alpha^{\beta}_{t_m}}{\arg\min} \sum_{n=1}^{|\mathcal{B}_{t_m}(\beta)|}\left(V_{t_{m+1}}(\mathbf{S}^{\beta}_{t_{m+1}}(n)) - \sum_{k=1}^{K}\alpha^{\beta,k}_{t_m}(k)\varphi_k(\mathbf{S}^{\beta}_{t_{m+1}}(n))\right)^2,$$

From this new equation it is evident that for each time step one more regression is needed, to compute the exposure under the $\mathbb{P}$ measure. Since this exposure value also depends on the early exercise policy these values should be computed backwards in time. As all the ingredients for this computation are in place during the SGBM valuation algorithm it can efficiently be computed during the initial valuation run, for a very small increase in computational costs.

Furthermore the regression target values used in the $\mathrm{EE}_{t_m}(t_u)$ computation should be reconsidered. The regression coefficient should now be calculated through a regression on the $\mathrm{E}^{\mathbb{P}}_{t_u}$ values and not the $V_{t_u} = \mathrm{E}^{\mathbb{Q}}_{t_u}$. So now the regression coefficients should satisfy

$$\underset{\alpha^{\beta}_{t_m,t_u}}{\arg\min} \sum_{n=1}^{|\mathcal{B}_{t_m}(\beta)|} \left(\mathrm{E}^{\mathbb{P}}_{t_u}(\mathbf{S}^{\beta}_{t_u}(n)) - \sum_{k=1}^{K} \alpha^{\beta,k}_{t_m,t_u}(k)\varphi_k(\mathbf{S}^{\beta}_{t_u}(n)) \right)^2 .$$

These coefficients are then plugged in into EE Equation 5.2.

5.4 Benefit of the hybrid measure

From the replicated results it can be observed that the use of the hybrid measure for the KVA term can result in a lower price than the $\mathbb{Q}$ measure. Due to the fact that the KVA term is based on the EEPE formula, which takes the integral of the maximum over increasing time intervals, this term can be lowered if the maximum of these intervals can be lowered. For this to happen the time t_m conditional EE profile under $\mathbb{P}$ should have lower maxima than the conditional EE profile under $\mathbb{Q}$.

Since the historically observed volatilities are usually lower than those implied by the market this will be assumed to be the case for the rest of this thesis, coinciding with market convention. Thus he fact that $\sigma_{\mathbb{P}} < \sigma_{\mathbb{Q}}$ gives that the option value under the historic volatility is lower. This is due to the fact that when the volatility is higher, the chance that the option ends up in-the-money is higher, and more likely with a greater payoff. Since this does not hold for the other end of the spectrum as these payoffs are all zero, it is evident that a lower volatility implies a lower price. This then results in a lower exposure each time step.

As a reference value for the KVA-SGBM output value a lower bound can be constructed by taking the maximum operator out of the expectation through use of Jensen's inequality

$$\begin{aligned} \mathrm{KVA}^{CCR}_0 &= \int_0^T c_t \int_t^{t+1Y} \mathbb{E}^{\mathbb{Q}} \left[\max_{u\in[t,s]} \mathbb{E}^{\mathbb{P}}[p_{0,t}\mathrm{E}_u|\mathcal{F}_t] \middle| \mathcal{F}_0 \right] dudt, \\ &\geq \int_0^T c_t \int_t^{t+1Y} \max_{u\in[t,s]} \mathbb{E}^{\mathbb{Q}} \left[\mathbb{E}^{\mathbb{P}}[p_{0,t}\mathrm{E}_u|\mathcal{F}_t] \middle| \mathcal{F}_0 \right] dudt. \end{aligned}$$

Then by considering there is only one measure the lower bound is approximated by

$$\begin{aligned} \widehat{\mathrm{KVA}}^{\mathbb{A}}_0 &\approx \int_0^T c_t \int_t^{t+1Y} \max_{u\in[t,s]} \mathbb{E}^{\mathbb{A}} \left[\mathbb{E}^{\mathbb{A}}[p_{0,t}\mathrm{E}_u|\mathcal{F}_t] \middle| \mathcal{F}_0 \right] dudt, \\ &= \int_0^T c_t \int_t^{t+1Y} \max_{u\in[t,s]} \mathbb{E}^{\mathbb{A}}[p_{0,t}\mathrm{E}_u \middle| \mathcal{F}_0 \Big] dudt. \end{aligned}$$

This approximation freezes the EE_{t_0}-profile and using it subsequently for all the further time steps, successfully eliminating the hybrid measure problem. Note that this is only a lower bound for $\mathbb{A} \equiv \mathbb{Q} \sim \mathbb{P}$.

5.5 Cases

For the case study the impact of the maturity time, moneyness and volatility on the KVA charge will be analysed for the three different Bermudan options described in the previous chapter. The tests are all setup with the following settings:

- The algorithm is run 30 times. The results are averaged and the standard deviation of these values is estimated.
- The market is assumed to be stressed, thus the implied volatility is greater than the historical volatility, and the PD intensity is modelled with $\bar{h} = 0.1$.
- The algorithm is run for $N = 5 \cdot 10^5$ Monte Carlo sample paths, with monthly exercise and observation times, $\Delta t = \frac{1}{12}$.
- The algorithm is run with $\nu = 16$ for the Black and Scholes Bermudan put, both single and multidimensional as convergence for this amount of bundles has been established in Chapter 4. For the Heston case the number of bundles is significantly increased to $\nu = 128$ by the same argument.

5.5.1 The Black and Scholes model test case

The first test case considers a monthly Bermudan put option on a stock which has an implied volatility $\sigma_{\mathbb{Q}} = 0.4$, a historical volatility of $\sigma_{\mathbb{P}} = 0.3$, and uses the USD 12-month LIBOR of $r = 0.00277$. The initial price is set to be $S_0 = 100$. The effects of the moneyness on the KVA of the the Bermudan put option are tested for three levels of moneyness: in-the-money, at-the-money and out-of-the-money, with strikes of 80%, 100% and 120% of the initial price respectively.

	$T = 0.5$			$T = 1$			$T = 1.5$		
Moneyness	$\mathrm{KVA}_0^{\mathbb{QP}}$	$\mathrm{KVA}_0^{\mathbb{Q}}$	$\widehat{\mathrm{KVA}}_0^{\mathbb{Q}}$	$\mathrm{KVA}_0^{\mathbb{QP}}$	$\mathrm{KVA}_0^{\mathbb{Q}}$	$\widehat{\mathrm{KVA}}_0^{\mathbb{Q}}$	$\mathrm{KVA}_0^{\mathbb{QP}}$	$\mathrm{KVA}_0^{\mathbb{Q}}$	$\widehat{\mathrm{KVA}}_0^{\mathbb{Q}}$
ITM	0.0718 (0.0001)	0.0805 (0.0001)	0.0800 (0.0001)	0.3412 (0.0005)	0.3651 (0.0005)	0.3590 (0.0005)	0.7767 (0.0010)	0.8213 (0.0012)	0.8004 (0.0012)
ATM	0.0395 (0.0000)	0.0437 (0.0000)	0.0437 (0.0000)	0.2132 (0.0002)	0.2265 (0.0002)	0.2242 (0.0002)	0.5258 (0.0004)	0.5525 (0.0005)	0.5444 (0.0005)
OTM	0.0113 (0.0000)	0.0129 (0.0000)	0.0129 (0.0000)	0.0916 (0.0001)	0.0980 (0.0001)	0.0973 (0.0001)	0.2687 (0.0002)	0.2825 (0.0002)	0.2799 (0.0002)

Table 5.1: The hybrid measure KVA values compared with the $\mathbb{Q}$-measure and the frozen EE KVA.

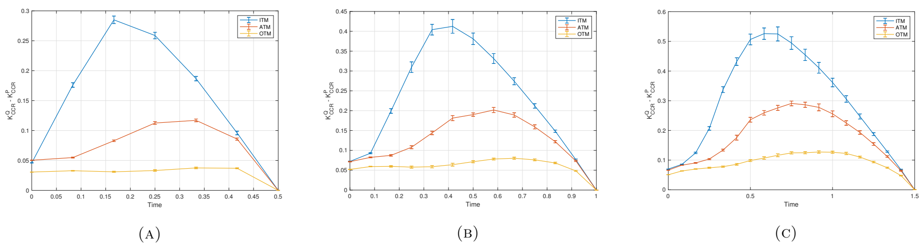

Figure 5.4: The difference between the $K^{\mathbb{Q}}_{CCR}$ and $K^{\mathbb{P}}_{CCR}$ values for each moneyness and maturity.

From Figure 5.4 A where the relative difference between the regulatory capital values calculated under the $\mathbb{P}$ and $\mathbb{Q}$, it is evident that the hybrid measure case is certainly not trivial, as there is an apparent difference present in the K_{CCR} values, for the Bermudan put option test case. That this use of a hybrid measure has a positive impact on the KVA price can be seen from Table 5.1. There it is shown that the hybrid measure reduces the KVA for every level of moneyness and maturity length.

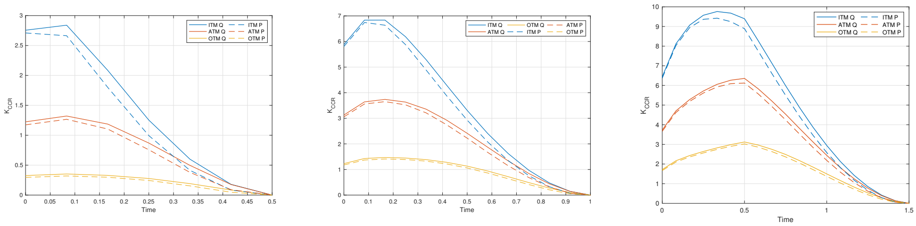

(A) (B) (C)

Figure 5.5: The $K^{\mathbb{Q}}_{CCR}$ and $K^{\mathbb{P}}_{CCR}$ values for the three different levels of moneyness.

In Figure 5.5 the combined impact of the EEPE's time horizon and the PD intensity process are displayed, in the third panel. For the first two panel the time horizon spans the complete duration of the option. However, for a maturity of $T = 1.5$ this changes. From the $t = 0.5$ marker the increase in the K_{CCR} becomes less or even starts to decay, which results in a slower growth of the KVA for higher maturities. This change can be ascribed to the EEPEś time horizon since the Unconditional EE profiles are very similar and do not exhibit this decay, see Figure 5.6.

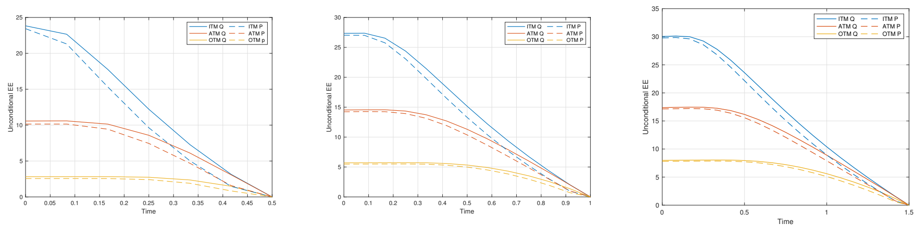

(A) (B) (C)

Figure 5.6: The unconditional $EE^{\mathbb{Q}}$ and $EE^{\mathbb{P}}$ values for the three different levels of moneyness.

5.6 The Heston model test case

The second test case to verify the KVA computation algorithm considers again a monthly Bermudan put option, but this time the underlying dynamics are governed by Heston model dynamics. The instantaneous implied volatility is $v_0^{\mathbb{Q}} = 0.1$ while the instantaneous historical volatility is $v_0^{\mathbb{P}} = 0.05$. The other Heston model parameters are the mean-reversion $\kappa = 2$, the volatility of the volatility $\gamma = 0.3$, the correlation $\rho = -0.6$ and the spot price $S_0 = 10$. Furthermore the USD 12-month LIBOR is used with $r = 0.00277$. The model is run for three levels of moneyness of 80%, 100% and 120% of the spot price.

	$T = 0.5$			$T = 1$			$T = 1.5$		
Moneyness	$\text{KVA}_0^{\mathbb{QP}}$	$\text{KVA}_0^{\mathbb{Q}}$	$\widehat{\text{KVA}}_0^{\mathbb{Q}}$	$\text{KVA}_0^{\mathbb{QP}}$	$\text{KVA}_0^{\mathbb{Q}}$	$\widehat{\text{KVA}}_0^{\mathbb{Q}}$	$\text{KVA}_0^{\mathbb{QP}}$	$\text{KVA}_0^{\mathbb{Q}}$	$\widehat{\text{KVA}}_0^{\mathbb{Q}}$
ITM	0.0521 (0.0001)	0.0423 (0.0001)	0.0515 (0.0001)	0.2308 (0.0003)	0.2023 (0.0003)	0.2234 (0.0003)	0.4332 (0.0007)	0.4843 (0.0007)	0.4582 (0.0006)
ATM	0.0312 (0.0000)	0.0277 (0.0000)	0.0314 (0.0000)	0.1551 (0.0002)	0.1442 (0.0002)	0.1539 (0.0002)	0.3627 (0.0004)	0.3407 (0.0005)	0.3546 (0.0004)
OTM	0.0076 (0.0000)	0.0065 (0.0000)	0.0076 (0.0000)	0.0619 (0.0001)	0.0569 (0.0001)	0.0614 (0.0001)	0.1799 (0.0002)	0.1694 (0.0002)	0.1762 (0.0002)

Table 5.2: The hybrid measure KVA values compared with the $\mathbb{Q}$-measure and the frozen EE KVA.

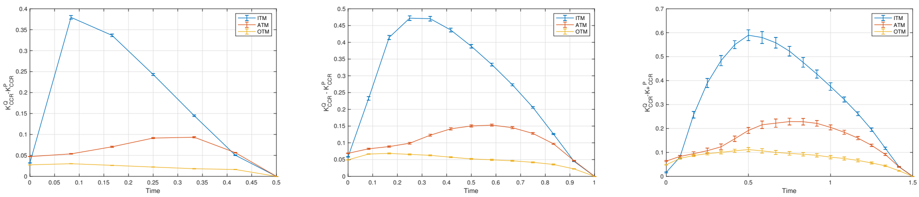

(A) (B) (C)

Figure 5.7: The difference between the $\text{K}_{CCR}^{\mathbb{Q}}$ and $\text{K}_{CCR}^{\mathbb{P}}$ values for each moneyness and maturity.

Regarding Figure 5.7, the difference in regulatory capital between the values, calculated by the hybrid historical parameters and the implied Heston parameters, is again present for the Bermudan put option with the Heston model dynamics for the underlying asset. This coincides with the results presented in Table 5.2. In that Table it is evident that the use of the hybrid $\mathbb{P}$ in $\mathbb{Q}$ measure results in a systematically lower KVA value than the values obtained through the implied volatility measure.

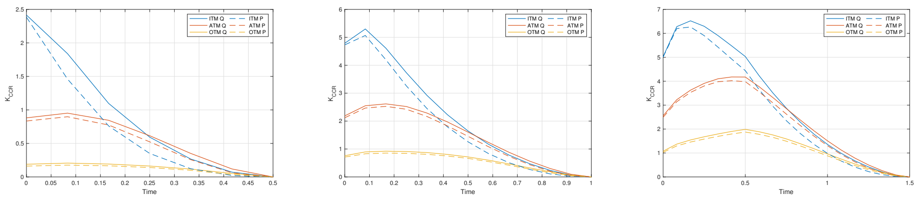

(A) (B) (C)

Figure 5.8: The $\text{K}_{CCR}^{\mathbb{Q}}$ and $\text{K}_{CCR}^{\mathbb{P}}$ values for the three different levels of moneyness.

As was previously seen in the Black and Scholes test case it also holds for the Heston test case that the origin of the difference between the hybrid measure and the single $\mathbb{Q}$ measure KVA pricing lie in the EE calculation, see Figures 5.8 and 5.9.

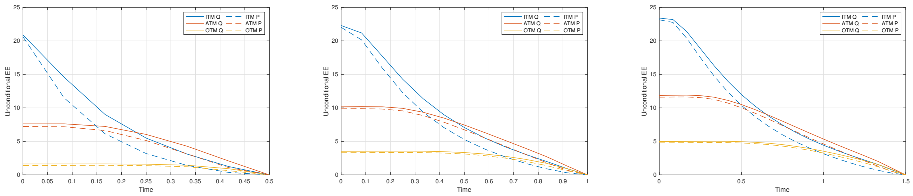

(a) (b) (c)

Figure 5.9: The unconditional $EE^{\mathbb{Q}}$ and $EE^{\mathbb{P}}$ values for the three different levels of moneyness.

5.7 Conclusion

This chapter has successfully shown that it is possible to apply the KVA-SGBM for hybrid measure KVA calculations to the problem of Bermudan option pricing under both the Black and Scholes model and the Heston model. By incorporating the early-exercise effects of the Bermudan option into the exposure calculations the KVA-SGBM algorithm can efficiently price the regulatory capital charge related to the CCR.

From the results in this chapter it is clear that the hybrid measure calculation has an advantage over the $\mathbb{Q}$ measure calculation. As was shown, the $\mathbb{Q}$ measure estimation overestimation of the cost of the regulatory capital related to the option. This is lowered when the $\mathbb{P}$ measure is incorporated through the use of the historical volatility, noted that this is volatility should lower than the implied volatility.

This effect is explained by the fact that when the volatility is higher, the probability of the option ending up in-the-money is higher, and when this occurs it is likely to exceed the strike price by a greater amount. On the other side of this also hold for the out-of-the-money case. However, since the payoff value will be zero and does not depend on the level of out-of-the-moneyness this effect is thus limited. This leads to the option to have an increased value for an increased volatility.

For this thesis it was attempted to create another reference value through the use of the fully nested Monte Carlo algorithm. The preliminary results showed that the KVA values were quite comparable however the nested algorithm was still suffering from substantial standard deviations. Since KVA calculation through use of both the single measure and the frozen EEPE approaches already provided good reference values and due to the severe computational costs of the nested algorithm when applied to Bermudan option pricing these calculations are not included.

VI

Conclusion and outlook

6.1 Conclusion

This thesis reviewed the application of the SGBM to the pricing of the counterparty credit risk part of the KVA term as proposed in literature, [JKK17], and applied this technique to the example problem of Bermudan option pricing. After starting with the definition of the mathematical framework in which the value adjustments can be priced and the construction of the KVA terms, two numerical methods, the SGBM and as a benchmark the LSM, were presented to price Bermudan options under both Black and Scholes and Heston dynamics. These methods were then compared against each other and the convergence of the SGBM with respect to the number of bundles and basis functions has been demonstrated. For the LSM the convergence with respect to number of Monte Carlo paths, choice of - and number of basis functions.

The new part of this thesis has been the contribution of a case study performed on Bermudan options. The original algorithm proposed in literature has been generalised to also include Bermudan style derivatives through the alteration of the initial assumptions. The case study proved that the pricing of KVA under the $\mathbb{Q}$ compared to the pricing under the hybrid $\mathbb{P}$ in $\mathbb{Q}$ measure is certainly not trivial. The test cases of the modified algorithm has shown that the use of a hybrid measure to price KVA could produce beneficial results for Bermudan option pricing, as the hybrid measure KVA price is lower.

6.2 Outlook

Very little has been written about the calculation of the other KVA terms related to the credit valuation adjustment, CVA, and the market risk, MR. There is no literature yet on the computation of these terms through the efficient Greek calculation of the SGBM. In [GKD14] Kenyon and Green refer to [GK15] to use two techniques to calculate these two other KVA terms. It would be an interesting point to apply the SGBM for these calculations and offer an alternative to their proposed techniques since the SGBM is a highly efficient algorithm.

I

Appendix - A

A.1 Black and Scholes Geometric Average

Under GBM dynamics the asset prices are governed by

$$dS_t^i = rS_t^i dt + S_t^i \sigma_i dW_t^i, i = 1, ..., d.$$

Where W_t^i is a Brownian motion, the correlation is $dW_t^i dW_t^j = \rho_{ij} dt$, r is the risk-free rate and σ_i the volatility. For the construction of the characteristic function a transition is made to the log-process $X_t^i = \log(S_t^i)$, which results in

$$dX_t^i = (r - \frac{\sigma_i^2}{2})dt + \sigma_i dW_t^i.$$

For this process $\mathbf{X}_{t_m}$ is, given $\mathbf{X}_{t_{m-1}}^i$, bivariate normally distributed,

$$\mathbf{X}_{t_m} \sim \mathcal{N}(\mathbf{X}_{t_{m-1}} + \mu, \Sigma)$$

The characteristic function of then is given by

$$\begin{aligned}
\phi(u; t_m, t_{m+1}, \mathbf{X}_{t_m}) &= e^{i\boldsymbol{\mu}\mathbf{u} - \frac{1}{2} u \boldsymbol{\Sigma} u}, \\
\boldsymbol{\mu} &= X_{t_m}^i + \frac{1}{d}(r - \frac{\sigma_i^2}{2})\Delta t, \\
\boldsymbol{\Sigma} &= \frac{1}{d^2} \sum_{i=1}^{d} \sum_{j=1}^{d} \rho_{i,j} \sigma_i \sigma_j \Delta t.
\end{aligned}$$

From this analytic formula the moments can be derived by using the relation defined in 4.4.2.

A.2 Heston

Under the Heston dynamics the asset prices are governed by

$$\begin{aligned}
dX_t &= (r - \frac{v_t}{2}) + \rho\sqrt{v_t} dW_t^1 + \sqrt{1 - \rho^2}\sqrt{v_t} dW_t^2, \\
dv_t &= \kappa(\theta - v_t)dt + \gamma\sqrt{v_t} dW_t^1.
\end{aligned}$$

For the one dimensional basis function

$$\varphi_k(X_t) = X_t^k, \quad k = 0, ..., K,$$

the expectation functions are defined as

$$\phi_k(X_t, v_t) = \mathbb{E}^{\mathbb{A}}[\varphi_k(X_t)|(X_{t-1}, v_{t-1})], \quad k = 0, ..., K.$$

These moments can then be constructed out of the characteristic function of the Heston model related to the one dimensional variable X_t defined as

$$\phi(u; t_m, t_{m+1}, X_{t_m}, v_{t_m}) = \mathbb{E}^{\mathbb{Q}}[e^{iuX_{t_{m+1}}}|(X_{t_m}, v_{t_m})].$$

Since the Heston model is a special case of an affine model, it has been shown, [DPS00], that the characteristic function has the log-linear form

$$\phi(u; t_m, tm+1, X_{t_m}, v_{t_m}) = e^{\tilde{A}(\Delta t) + \tilde{B}_1(\Delta t)X_{t_m} + \tilde{B}_2(\Delta t)v_{t_m})}.$$

where the coefficients are defined as

$$\begin{aligned}
\tilde{B}_1 &= iu, \tilde{B}_2 = \frac{1}{\gamma}(\kappa - iu\gamma\rho + D_1) - \frac{2D_1}{\gamma^2(1 - D_2 e^{-D_1 \Delta t})}, \\
\tilde{A} &= \frac{\kappa\theta}{\gamma^2}((\kappa - iu\gamma\rho - D_1)\Delta t - 2\log(\frac{1 - D_2 e^{-D_1 \Delta t)}}{1 - D_2}), \\
D_1 &= \sqrt{(\kappa - \gamma\rho iu)^2 + \gamma^2(u^2 + iu)}, \\
D_2 &= \frac{\kappa - \gamma\rho iu - D_1}{\kappa - \gamma\rho iu + D_1}.
\end{aligned}$$

From this analytic formula the moments can be derived by using the relation defined in 4.4.2.

References

[And08] Leif Andersen. Simple and efficient simulation of the heston stochastic volatility model. *Journal of Computational Finance*, 11(3):1–43, 2008.

[BCB11] June BCBS. Basel iii: A global regulatory framework for more resilient banks and banking systems. *Basel Committee on Banking supervision, Bank for International Settlements. Basel*, 2011.

[BG$^+$04] Mark Broadie, Paul Glasserman, et al. A stochastic mesh method for pricing high-dimensional american options. *Journal of Computational Finance*, 7:35–72, 2004.

[BK11] Christoph Burgard and Mats Kjaer. Partial differential equation representations of derivatives with counterparty risk and funding costs. *The Journal of Credit Risk*, 7(3):1–19, 2011.

[BK13] Christoph Burgard and Mats Kjaer. Funding costs, funding strategies. *Risk*, pages 82–87, 2013.

[BM95] Jérôme Barraquand and Didier Martineau. Numerical valuation of high dimensional multivariate american securities. *Journal of financial and quantitative analysis*, 30(3):383–405, 1995.

[BM11] Damiano Brigo and Massimo Morini. Close-out convention tensions. *Risk*, 24(12):74, 2011.

[BS73] Fischer Black and Myron Scholes. The pricing of options and corporate liabilities. *Journal of political economy*, 81(3):637–654, 1973.

[Cha08] Don M. Chance. *Essays in derivatives.* Wiley, 2008.

[DPS00] Darrell Duffie, Jun Pan, and Kenneth Singleton. Transform analysis and asset pricing for affine jump-diffusions. *Econometrica*, 68(6):1343–1376, 2000.

[Fen17] Qian Feng. *Advanced Estimation of Credit Valuation Adjustment.* PhD thesis, Technische Universiteit Delft, 2017.

[GK15] Andrew Green and Chris Kenyon. MVA: Initial Margin Valuation Adjustment by replication and Regression. *Risk*, 2015.

[GKD14] Andrew Green, Chris Kenyon, and Chris Dennis. Kva: capital valuation adjustment by replication. *Risk*, page 82, 2014.

[Gre11] Andrew Green. *XVA: Credit, Funding and Capital Valuation Adjustments.* Wiley, first edition edition, 2011.

[Hul93] John C. Hull. *Options, futures and other derivative securities.* Prentice-Hall International, 1993.

[JKK17] Shashi Jain, Patrik Karlsson, and Drona Kandhai. Kva, mind your p's and q's! *Available at SSRN: https://ssrn.com/abstract=2792956*, 2017.

[JO15] Shashi Jain and Cornelis W Oosterlee. The stochastic grid bundling method: Efficient pricing of bermudan options and their greeks. *Applied Mathematics and Computation*, 269:412–431, 2015.

[KP12] Steve Kummer and Christian Pauletto. The history of derivatives: A few milestones. In *EFTA Seminar on Regulation of Derivatives Markets*, 2012.

[LR16] Andrew Lesniewski and Anja Richter. Managing counterparty credit risk via BSDEs. *arXiv preprint arXiv:1608.03237*, 2016.

[LS01] Francis A Longstaff and Eduardo S Schwartz. Valuing american options by simulation: a simple least-squares approach. *The review of financial studies*, 14(1):113–147, 2001.

[Mat10] William S. Mathers. *Synthetic Real Estate Investment for the small investor*. CreateSpace Independent Publishing Platform, 2010.

[Øks03] Bernt Øksendal. Stochastic differential equations. In *Stochastic differential equations*, pages 65–84. Springer, 2003.

[Pen08] George Gaetano Pennacchi. *Theory of asset pricing*. Pearson/Addison-Wesley Boston, 2008.

[Pit10] Vladimir Piterbarg. Funding beyond discounting: collateral agreements and derivatives pricing. *Risk*, 23(2):97, 2010.

[RO12] Marjon J Ruijter and Cornelis W Oosterlee. Two-dimensional fourier cosine series expansion method for pricing financial options. *SIAM Journal on Scientific Computing*, 34(5):B642–B671, 2012.

[She14] Yanbin Shen. *Credit Value Adjustment for Multi-Asset Options*. PhD thesis, TU Delft, Delft University of Technology, 2014.

[SS06] Rüdiger Seydel and Rudiger Seydel. *Tools for computational finance*, volume 3. Springer, 2006.

[Tur10] K Turunen. Exposure at default models for counterparty credit risk under basel frameworks. *AALTO University, Faculty of Information and Natural Sciences Research Project*, 2010.

[WDH93] Paul Wilmott, Jeff Dewynne, and Sam Howison. *Option pricing: mathematical models and computation*. Oxford financial press, 1993.

[Wel11] N. Wellink. Nout wellink: Looking beyond the current reforms, speech. `https://www.bis.org/list/speeches/author_nout+wellink/index.htm`, 2011.